Nuclear Physics and Hadrontherapy.

Daniel CUSSOL

LPC Caen, ENSICAEN,Université de Caen Basse-Normandie, IN2P3/CNRS

September 16, 2011

Overview

Why hadrontherapy?

Cancer in France (2010 data)

- $\approx$ 300,000 new cases per year
- $\approx$ 150,000 radiotherapy (X-rays) per year

45% success

- 22% surgery
- 9% surgery + radiotherapy
- 9% radiotherapy only
- 5% chemotherapy

55% failure

- 18% local failure
- 37% metastases

Radiation therapies

Goals

- Minimize irradiation on healthy tissues
- Increase efficiency on the tumour

Means

- Ballistics
- Biological efficiency

Radiotherapy

- Intensity Modulated Radio-Therapy
- Cyberknife
- Tomotherapy
- Hadrontherapy (p, n, α, heavy ions)

A short history of hadrontherapy

- "Radiological Use of Fast Protons", R. R. Wilson, Radiology, 47:487-491 (1946)
- Berkeley (USA) 1954-1974, 1,000 patients, α, Ne, C, Si, Ar
- Berkeley (USA) 1975-1993 1,200 patients, Ne, C
- 1961-2002 collaboration between Berkeley and the Massachusetts General Hospital to develop the protontherapy.$\sim$ 9,116 patients.
- many protontherapy centers in USA since 1990.
- HIMAC (Japan) 1994, Treatment Center, $\sim$ 1,500 patients, C
- GSI (Germany) 1997-2007, Medical trials, spot scanning, $\sim$ 300 patients, C
- HIT (Germany) november 2009, Treatment Center, p, C

Hadrontherapy centers in the World

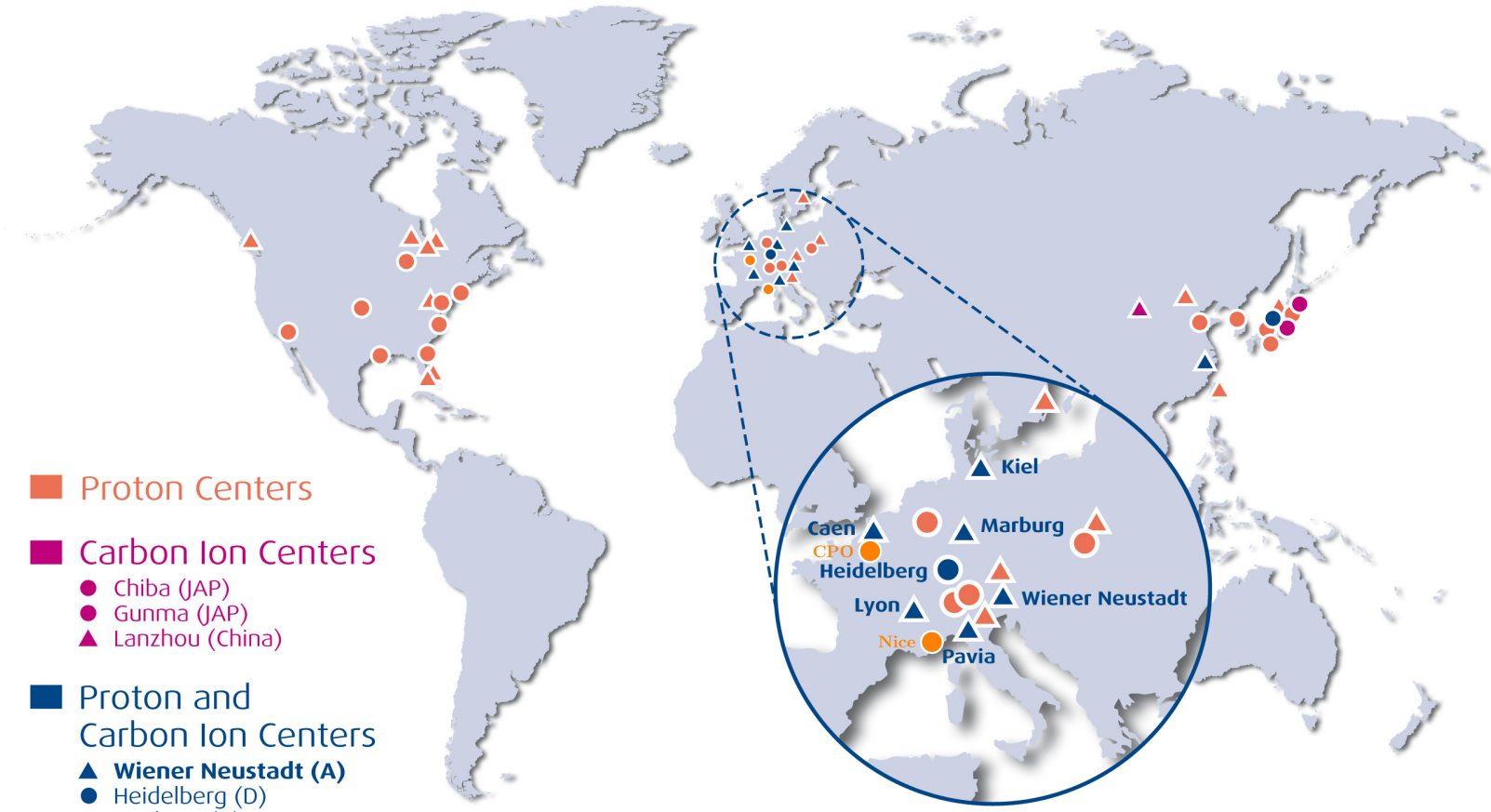

Ballistics

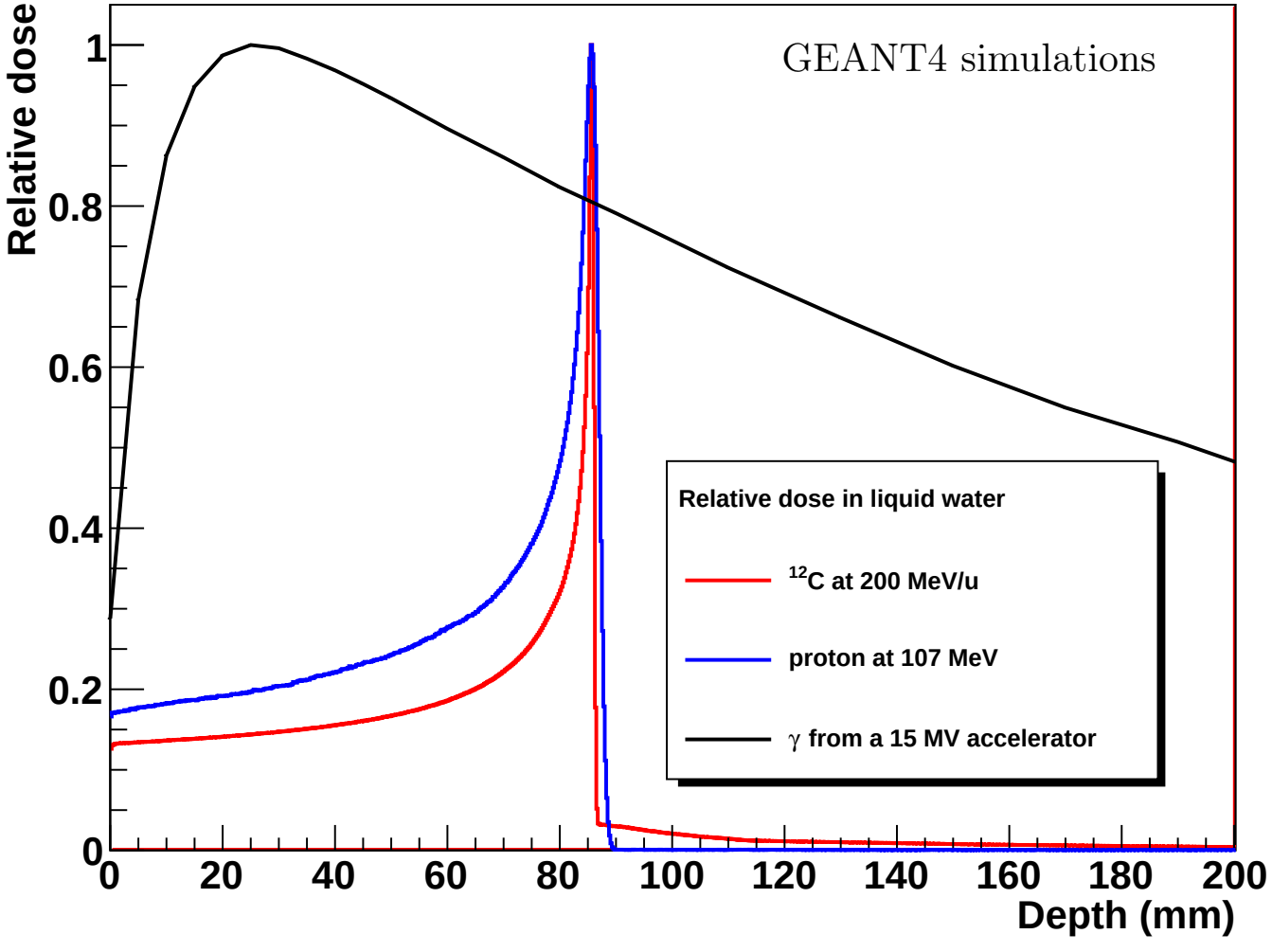
GEANT4 simulations
Relative dose
1
0.8
0.6
0.4
0.2
0
0
20
40
60
80
100
120
140
160
180
200
Depth (mm)
Relative dose in liquid water
^{12}C at 200 MeV/u
proton at 107 MeV
γ from a 15 MV accelerator

Relative Biological Efficiency

$$RBE_{iso} = \frac{D_\gamma}{D_{part}}$$

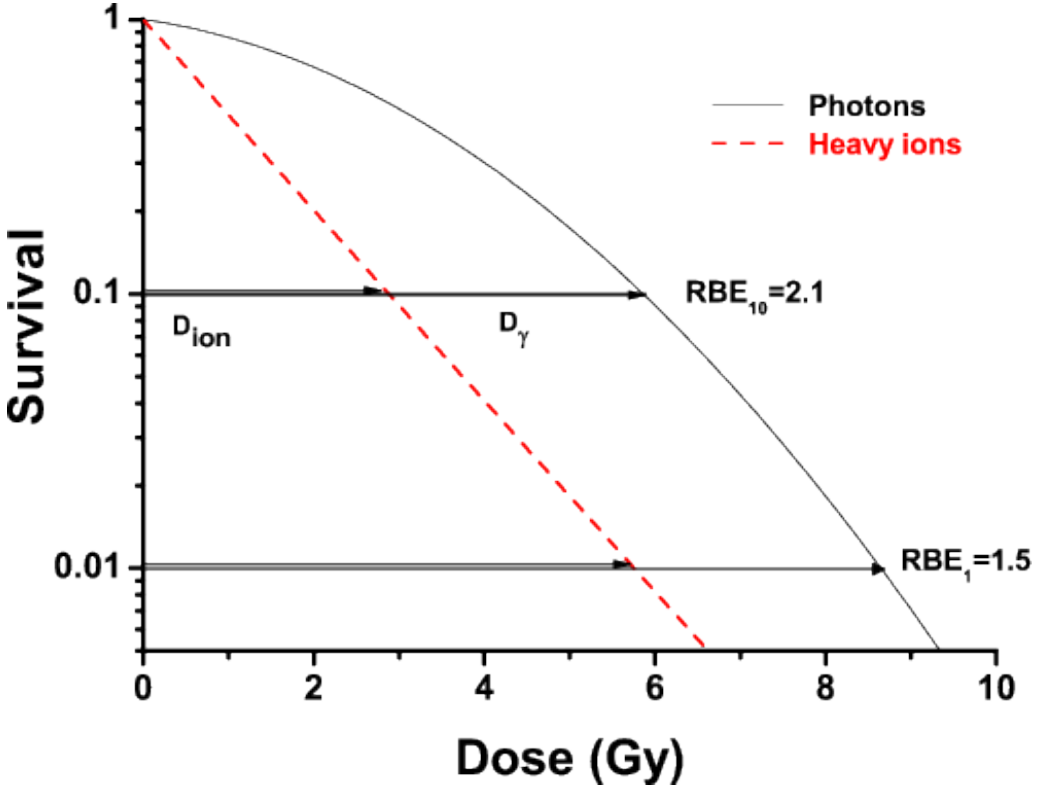

Oxygen Enhancement Ratio

$$OER = \frac{D_{hypoxic}}{D_{aerobic}}$$

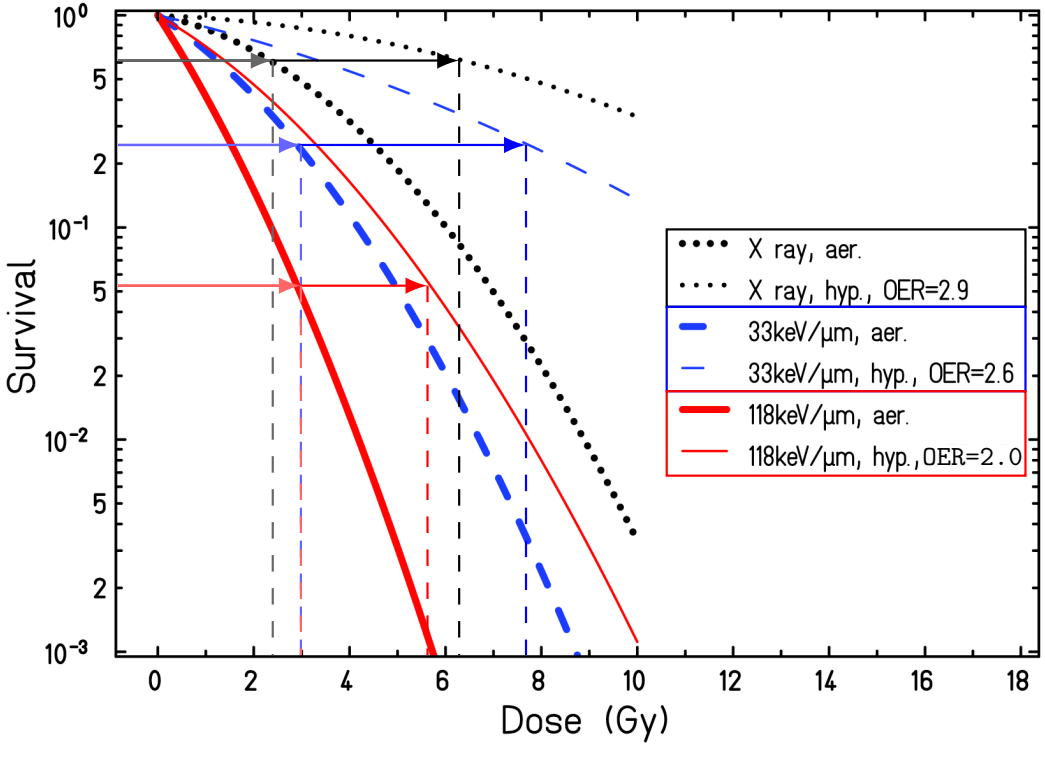

Biological effects

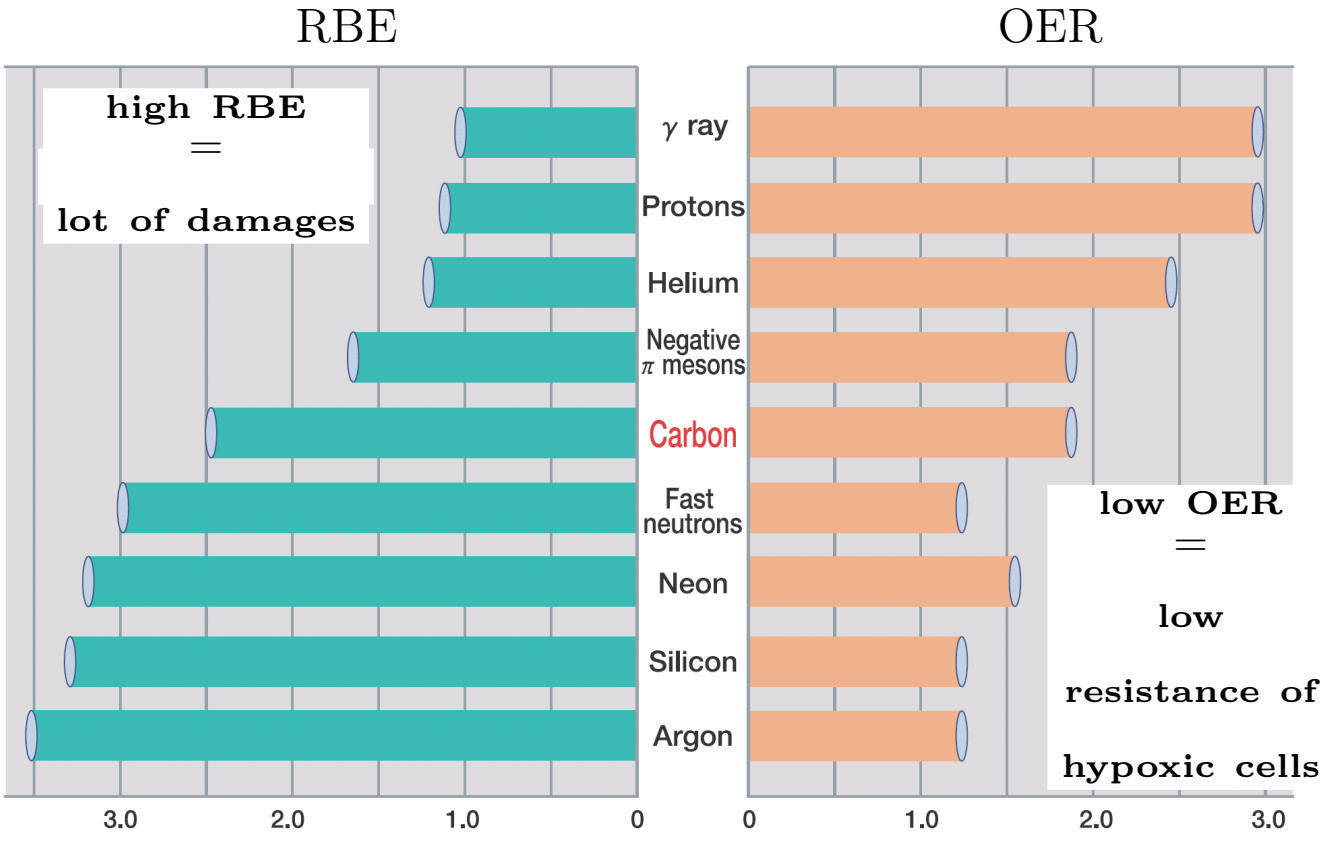

Indications for hadrontherapy

Main advantages

- Bragg Peak: accurate sighting of the tumour
- Low dose before the Bragg Peak: healthy tissues less irradiated
- Improved biological efficiency: better for radio-resistant tumours

Medical indications

Non operable and radio-resistant tumours: head and neck tumours, brain tumours.

the Treatment Planning System (TPS)

Treatment Planning System

A software to compute the parameters of the accelerator in order to deliver a given 3D dose map for:

- a given accelerator
- a given patient
- a given pathology

Existing TPS's

- **HIMAC** (Japan): Physical dose computed using , RBE taken ~ 2.
- **TRiP** (HIT, heidelberg): Physical dose computed using , RBE computed using the Local Effect Model (LEM) (Krämer and Scholz, 2000; Krämer et al., 2000)

A simple 1D example

The requirements

One wants to irradiate a 1cm large volume located 8cm in water. Summation of the contributions of many individual beams. For an individual beam i with incident energy E_i the dose $D_i(x)$ has been deposited at depth x. For a set of beams with different energies, the dose at depth x is given by: $D(x) = \sum_i N_i D_i(x)$. The biological dose is $D(x) = \sum_i N_i D_i(x) BF(x)$. The biological factor $BF(x)$ is equal to RBE for aerobic cells or is equal to $\frac{RBE}{OER}$ for hypoxic cells. The goal is to find the values of N_i to deposit a wanted biological dose $D_{wanted}(x)$ at depth x.

One solution

find the set of N_i values which minimizes the following quantity $\chi^2 = \int (D_{wanted}(x) - \sum_i N_i D_i(x) BF(x))^2 dx$

Physical Spread Out Bragg Peak (SOBP) for protons

Resolution

Solve the system of n equations with n unknown N_i values:

$$\frac{\partial \chi^2}{\partial N_i} = 0 \Rightarrow \int D(x) D_i(x) dx = \sum_j N_j \int D_j(x) D_i(x) dx$$

Weigths distribution for protons

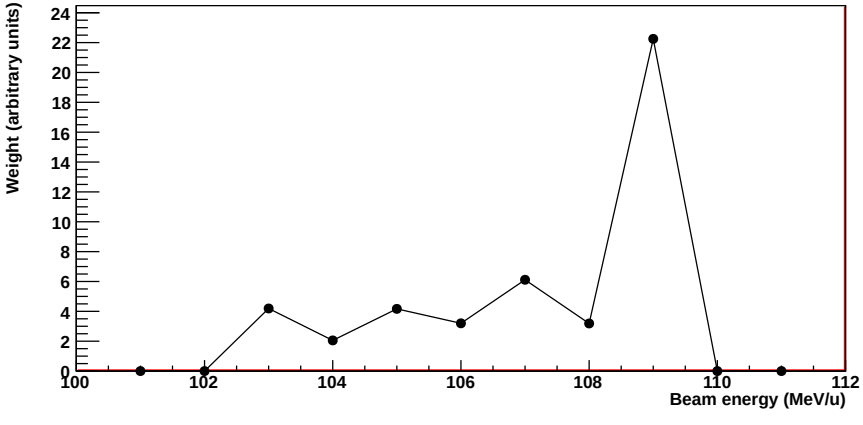

Spread Out Bragg Peak

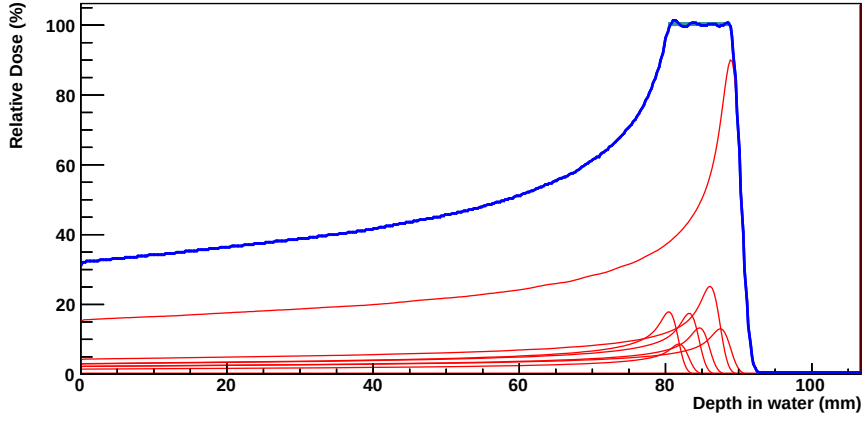

Physical SOBP for ^{12}C

Resolution

Solve the system of n equations with n unknown N_i values:

$$\frac{\partial \chi^2}{\partial N_i} = 0 \Rightarrow \int D(x) D_i(x) dx = \sum_j N_j \int D_j(x) D_i(x) dx$$

Weigths distribution for ^{12}C

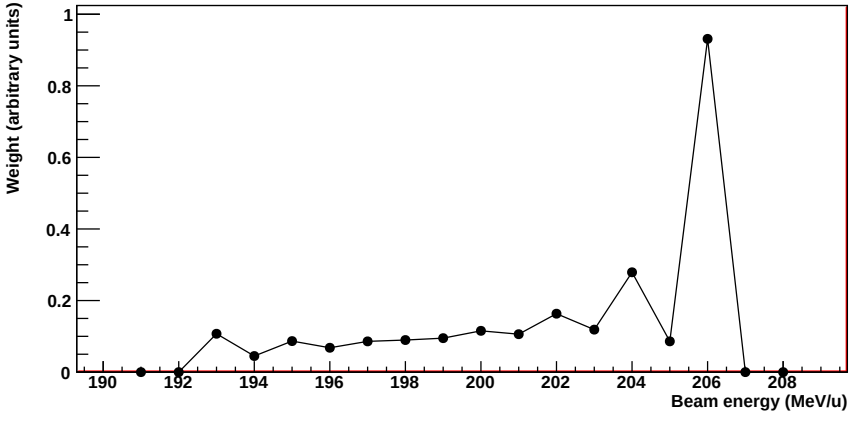

Spread Out Bragg Peak

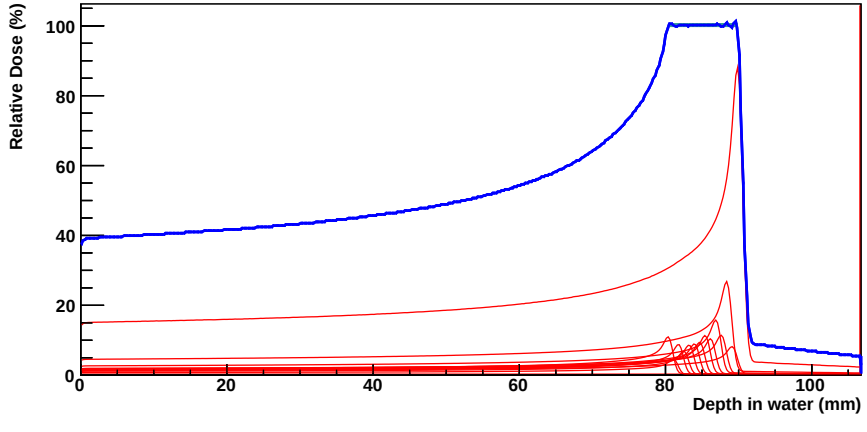

Simplified biological model

Relative Biological Efficiency

$$RBE = f(TEL) \approx f(\frac{dE}{dx})$$

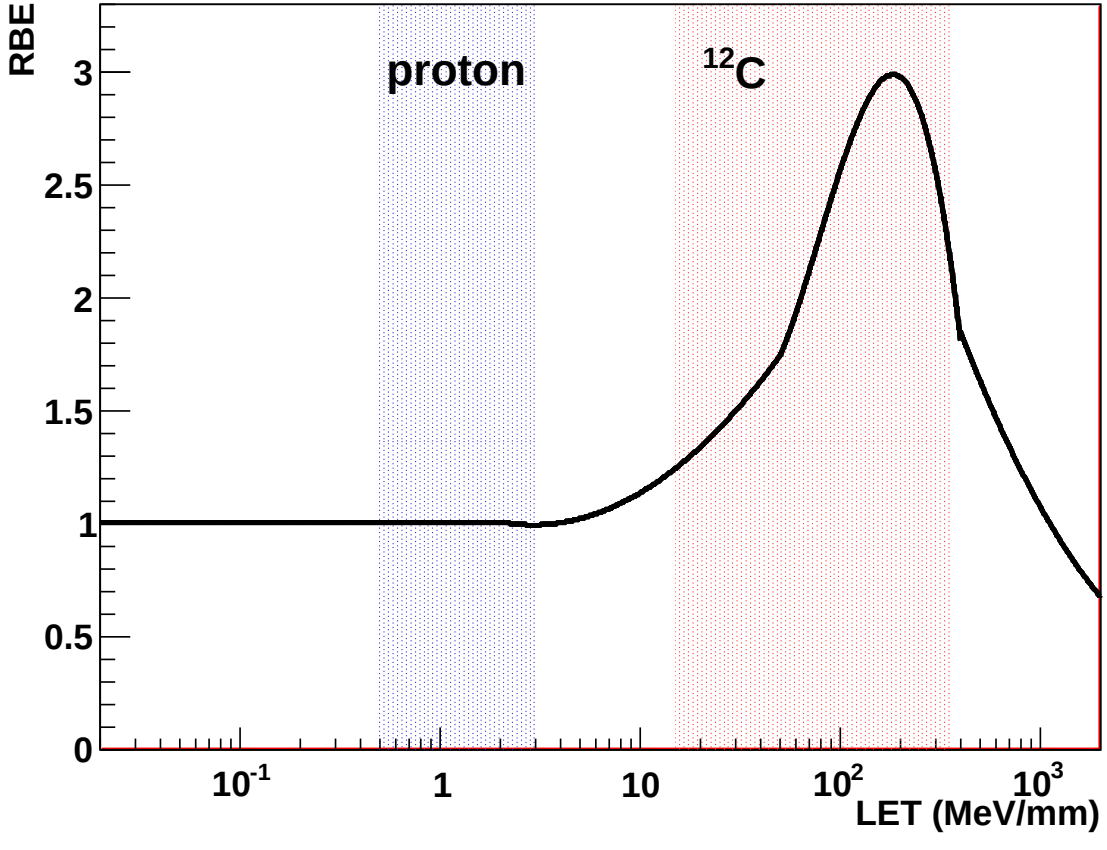

Biological SOBP for ^{12}C

Resolution

Solve the system of n equations with n unknown N_i values:

$$\int D(x)D_i(x)RBE_i(x)dx = \sum_j N_j \int D_j(x)RBE_j(x)D_i(x)RBE_i(x)dx$$

Weigths distribution for ^{12}C

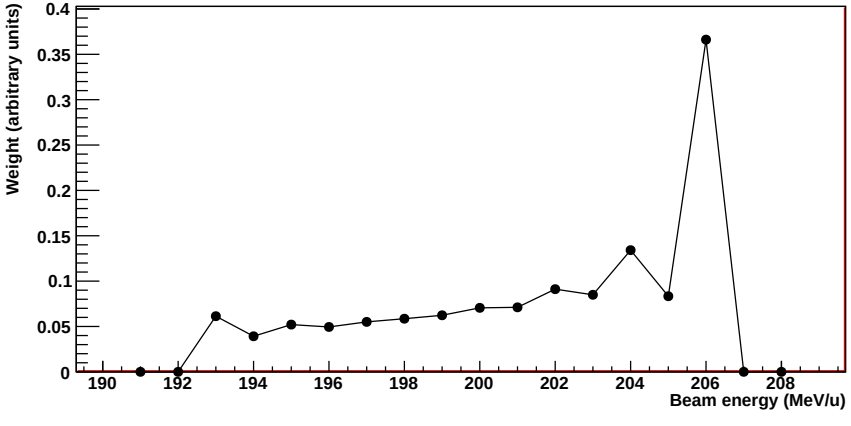

Spread Out Bragg Peak

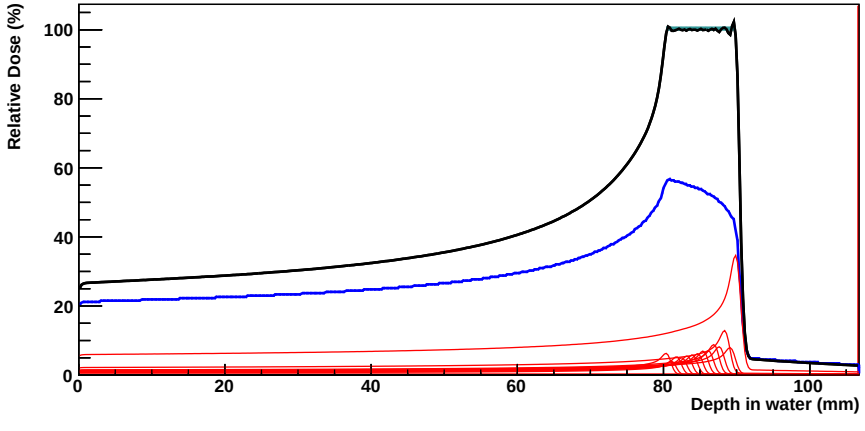

Passive beam delivery

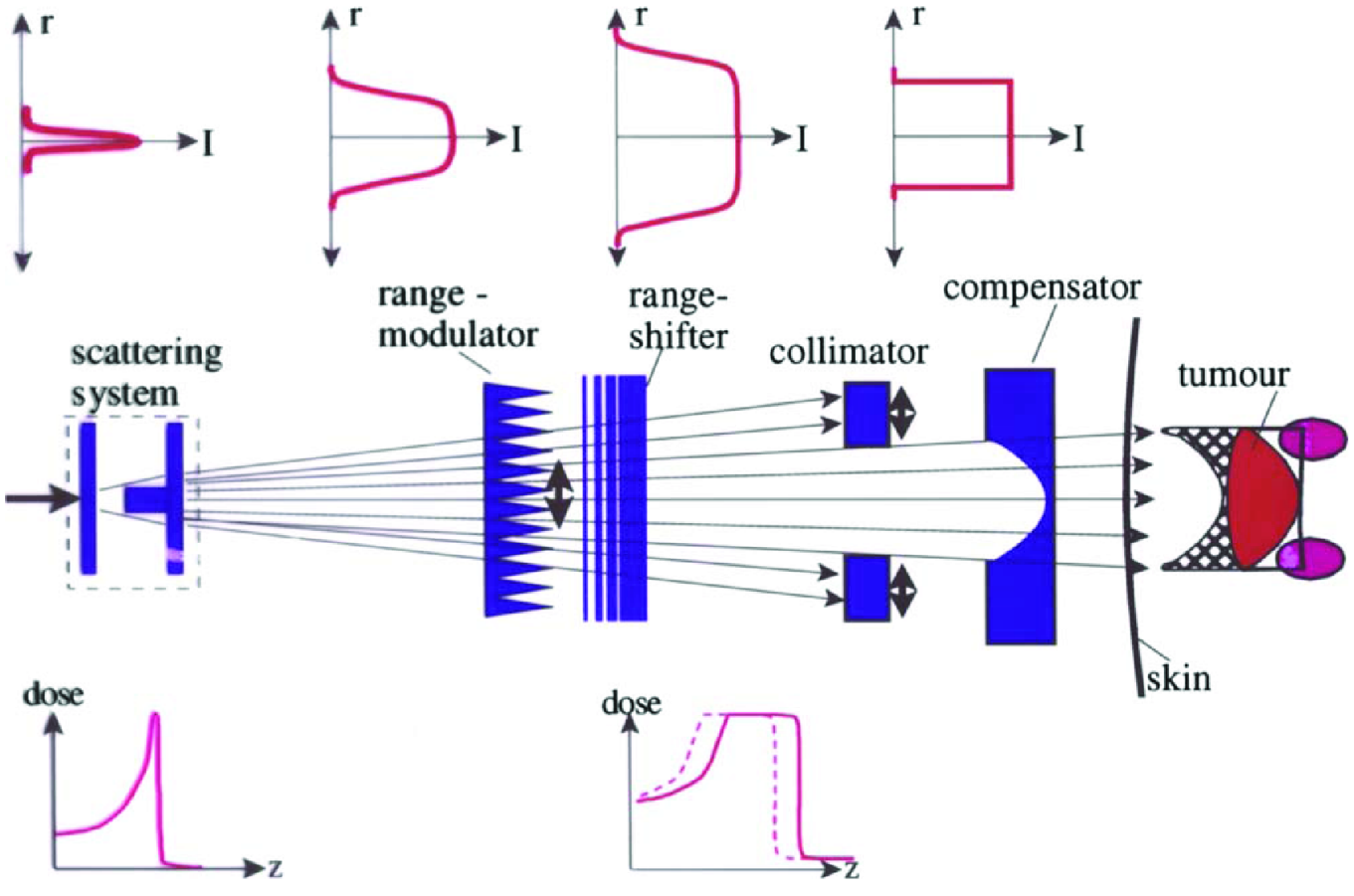

Active beam delivery (Spot scanning)

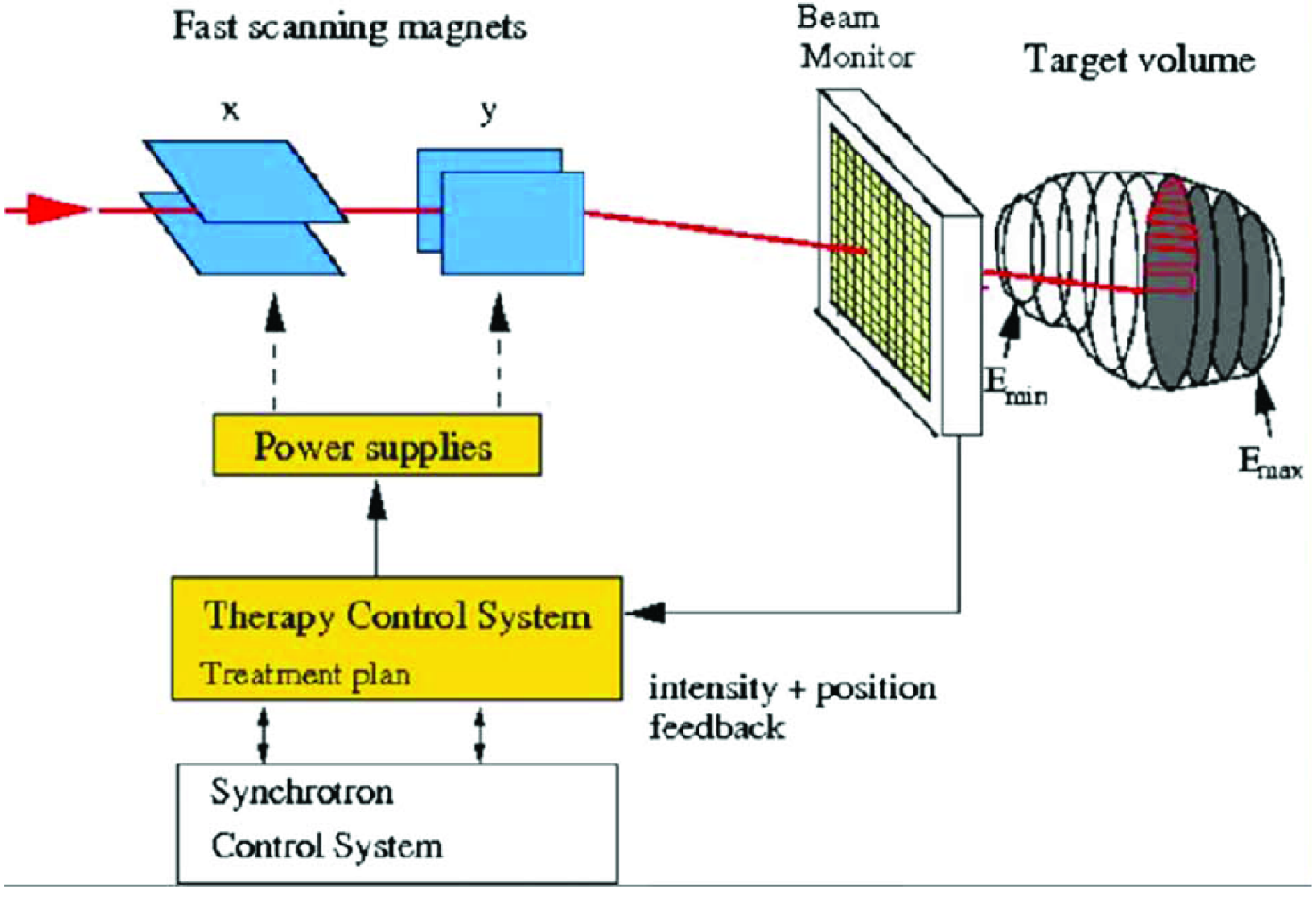

TPS Result (TRiP)

M.Krämer et al,
Phys. Med. Biol. 45 (2000) 3299–3317.

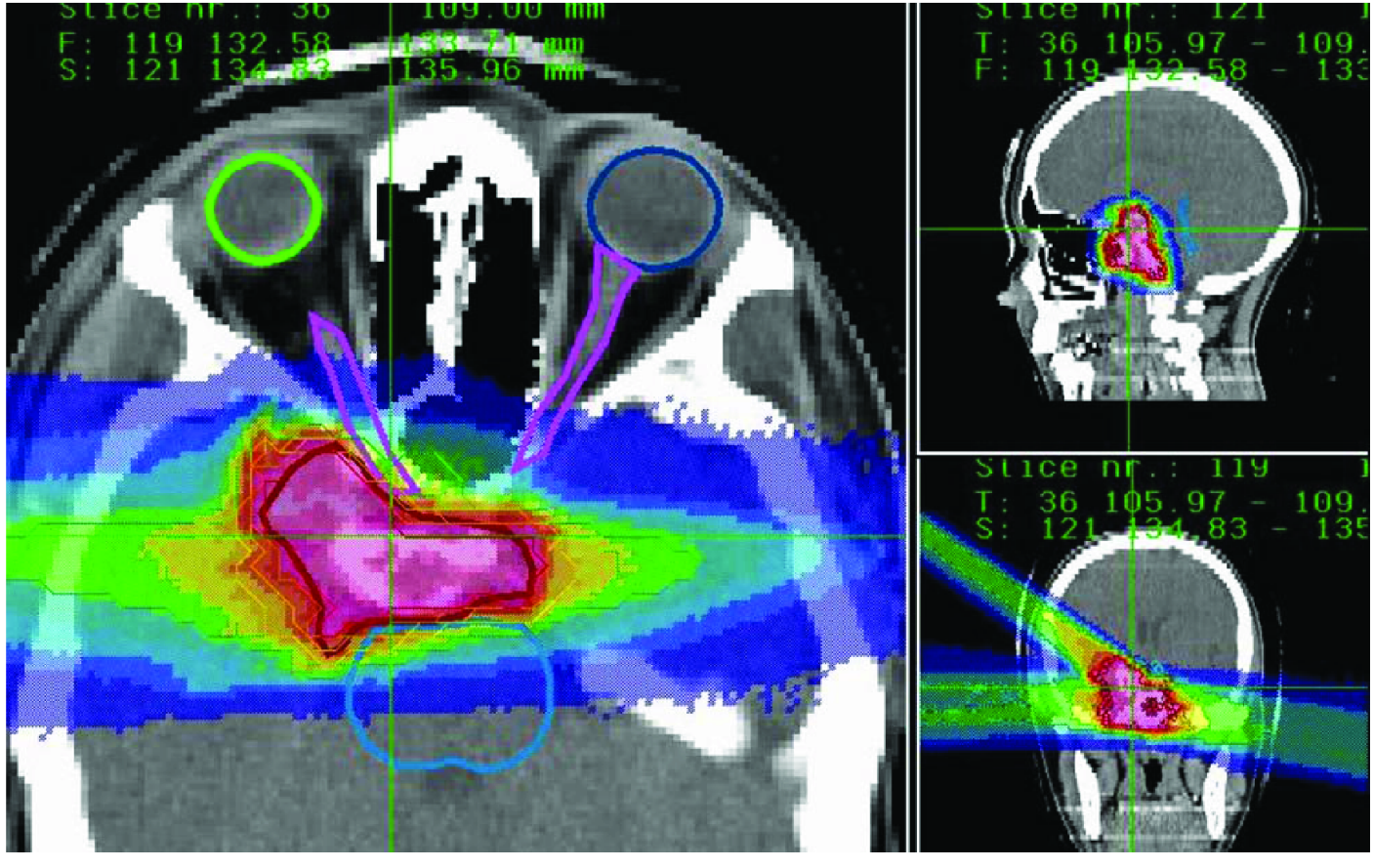

Dosimetry: Absorbed dose (ICRU60)

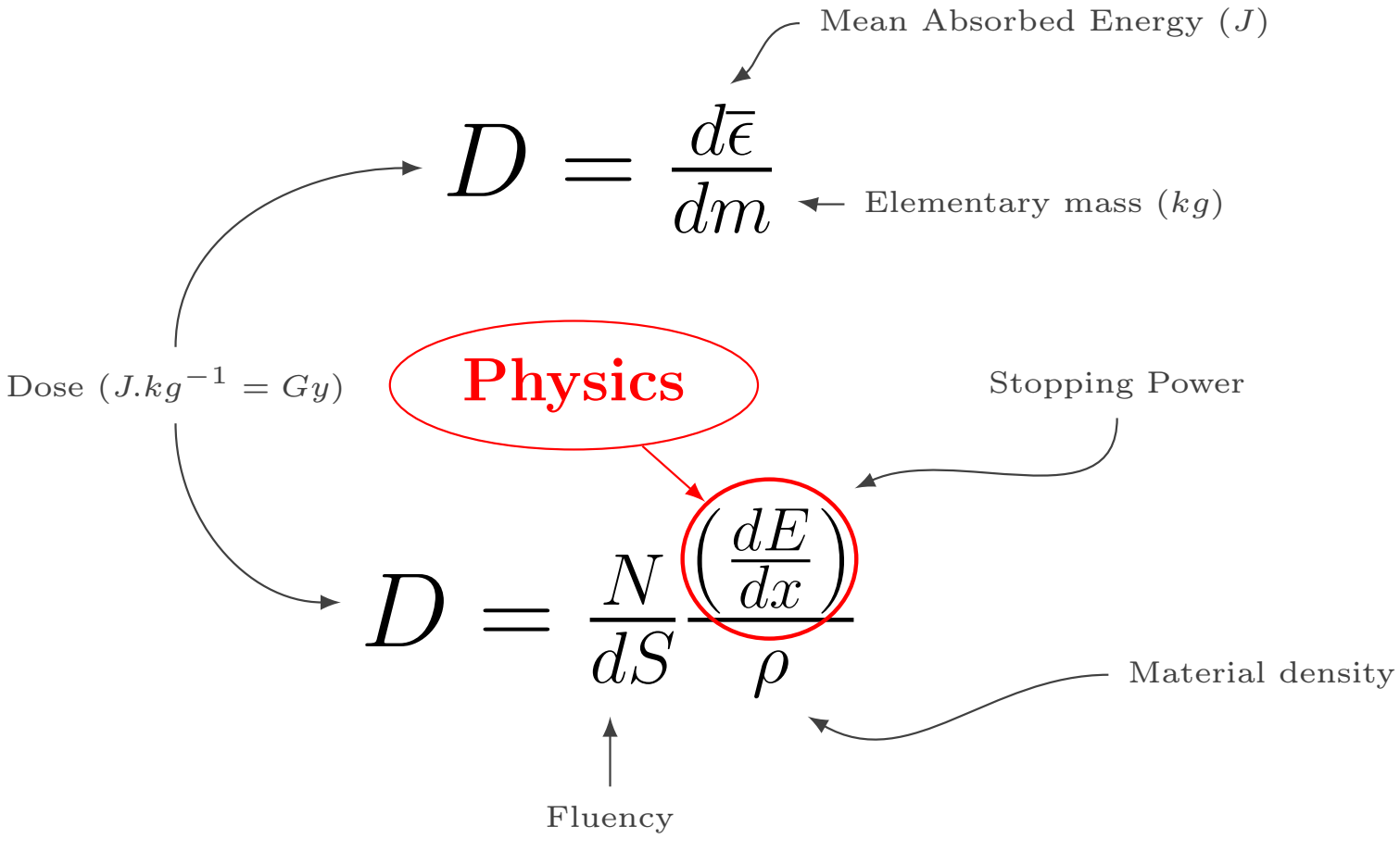

Main process: inelastic collisions with electrons

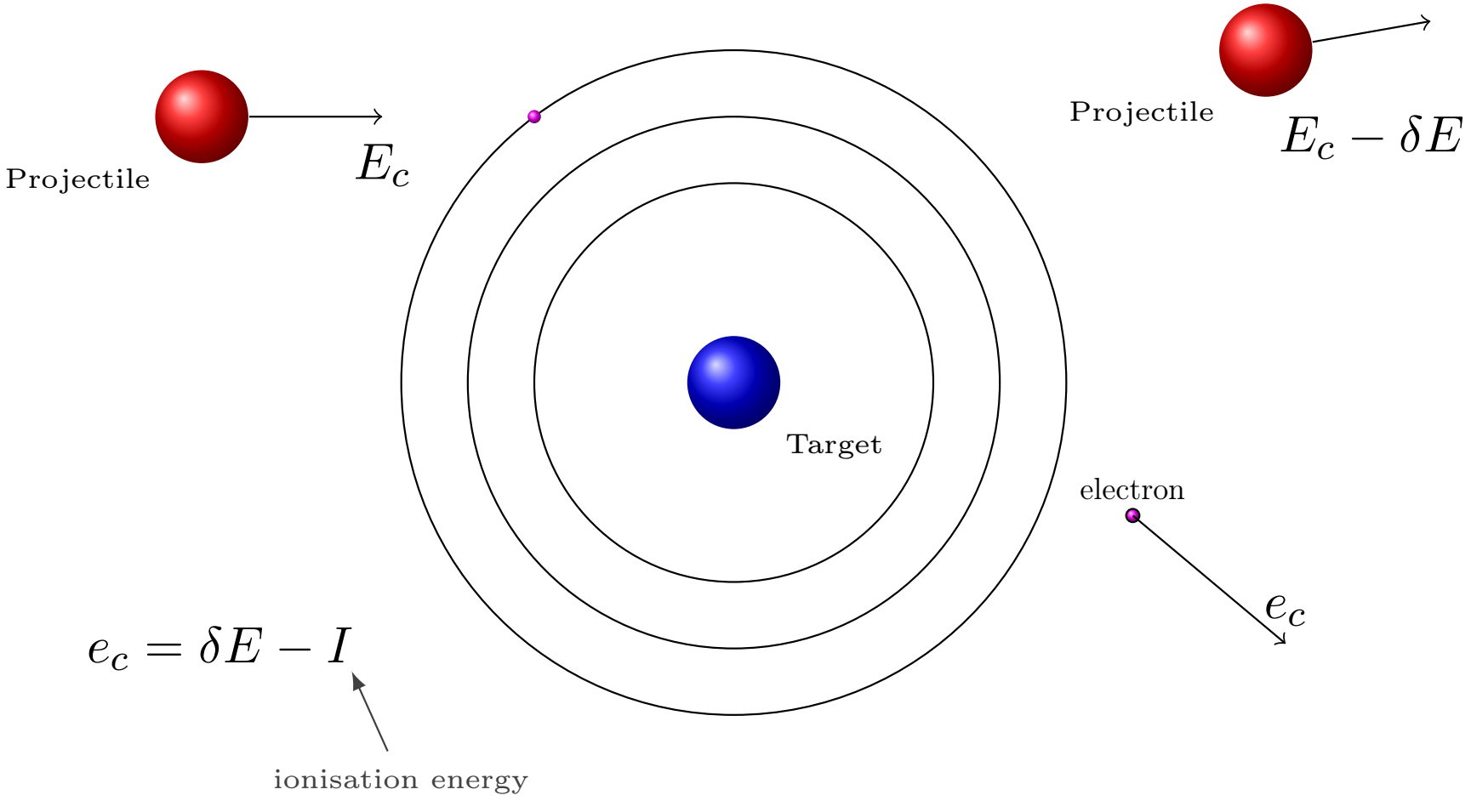

Some definitions

Stopping power

$\left(\frac{dE}{dx}\right)$: energy lost by the projectile per unit length.

Linear Energy Transfer

LET : energy transfered to the material per unit length.

$LET = \left(\frac{dE}{dx}\right) - \sum Ec(e_\delta)$

e_δ : electrons with a kinetic energy bigger than E_δ

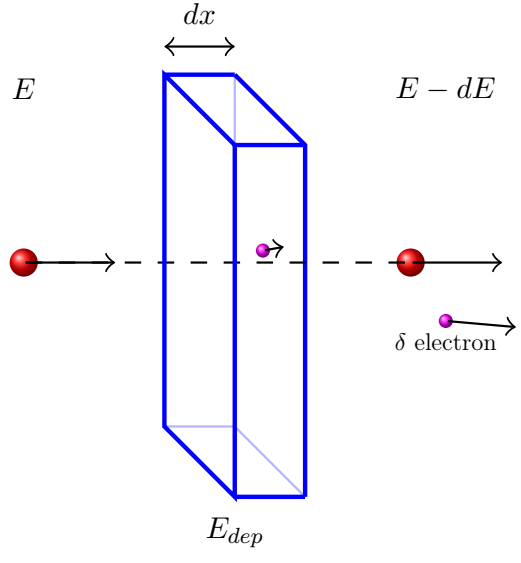

For heavy ions

$$\left(\frac{dE}{dx}\right) \approxeq LET \approxeq \frac{E_{dep}}{dx}$$

Typical LET values

GEANT4 simulations

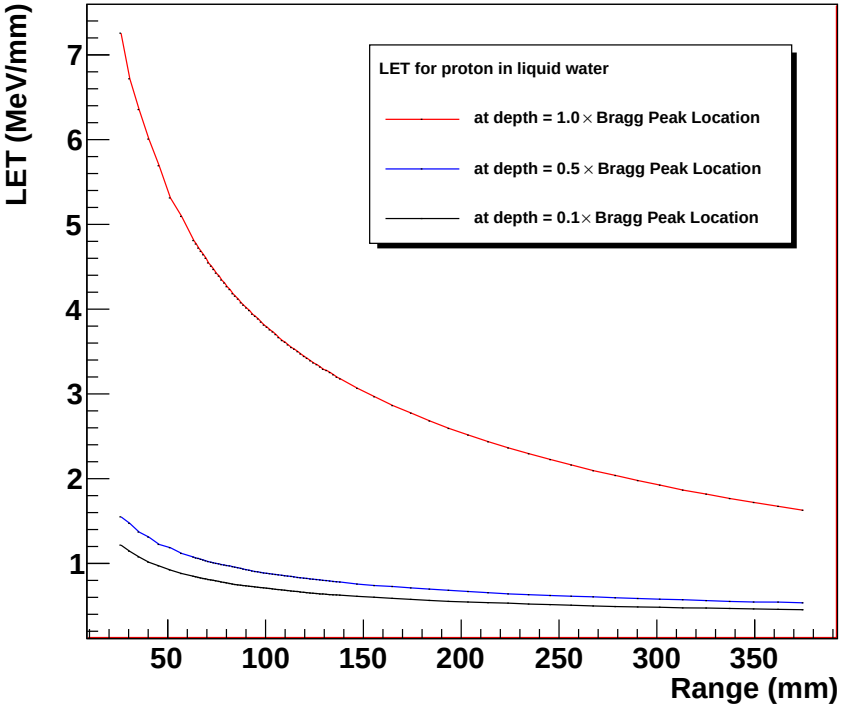

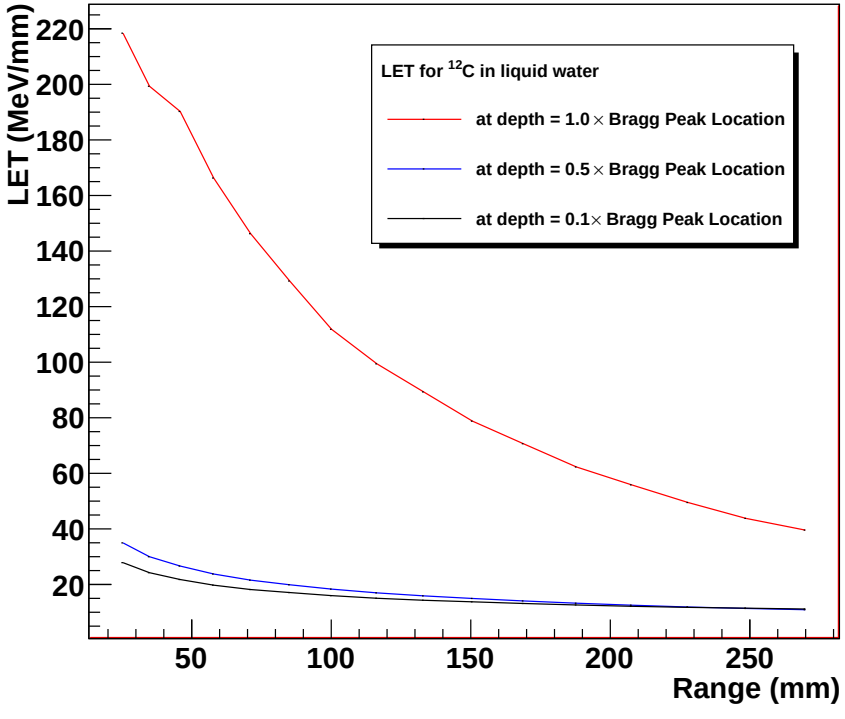

Numericals values

For protons

$\frac{dE}{dx} \approx 3\,MeV/mm$ at the Bragg Peak.

To deposit 1 Gy at the Bragg peak in liquid water ($\rho = 1\,mg/mm^3$):

$1\,Gy = \frac{N}{dS}\frac{3\,10^6 \times 1.6\,10^{-19}}{10^{-6}} \implies \frac{N}{dS} \approx 2\,10^6 protons/mm^2$

For ^{12}C

$\frac{dE}{dx} \approx 80\,MeV/mm$ at the Bragg Peak.

To deposit 1 Gy at the Bragg peak in liquid water ($\rho = 1\,mg/mm^3$):

$1\,Gy = \frac{N}{dS}\frac{80\,10^6 \times 1.6\,10^{-19}}{10^{-6}} \implies \frac{N}{dS} \approx 8\,10^4\,{}^{12}C/mm^2$

The Bethe-Bloch equation

Fano U., 1963, *"Penetration of protons, alpha particles, and mesons"*

Annu. Rev. Nucl. Sci. 13, 1–66.

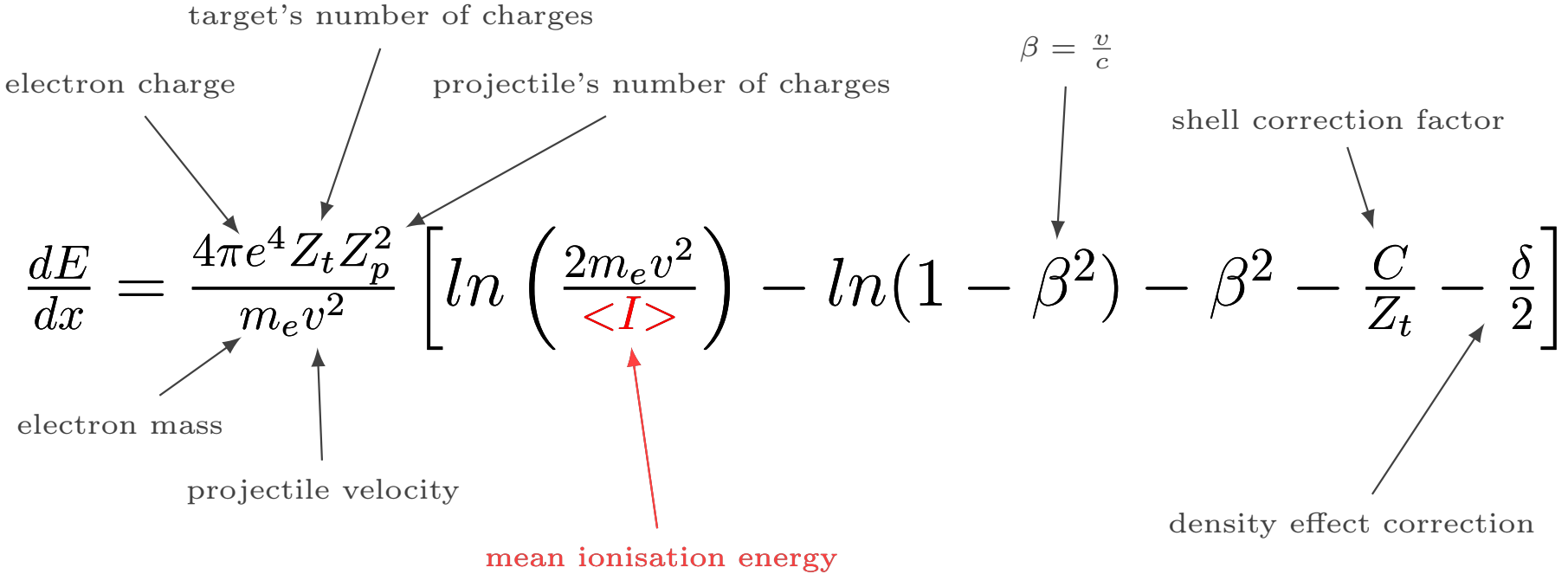

The Ionisation Energy

Computation from the chemical formula of the material

$$ln(< I >) = \left(\sum_i \frac{\omega_i Z_i}{A_i} ln(I_i)\right) / \left(\sum_i \frac{\omega_i Z_i}{A_i}\right)$$

where

- Z_i and A_i : charge and mass numbers for element i
- ω_i : proportion of element i in the material
- I_i : ionisation energy of element i from Janni tables

Fit to experimental data (liquid water)

- $< I >= 79.7\ eV$ from energy loss measurements with 70 MeV protons (Bichsel and Hiraoka, 1992; Bichsel et al., 2000).
- $< I >= 75 - 78\ eV$ from precision Bragg curve measurements for protons and various heavier ions (Kumazaki et al., 2007; Paul,2007; Schardt et al., 2008).
- $< I >= 75\ eV$ ICRU recommended value.

Effect on the $< I >$ value on the particle range

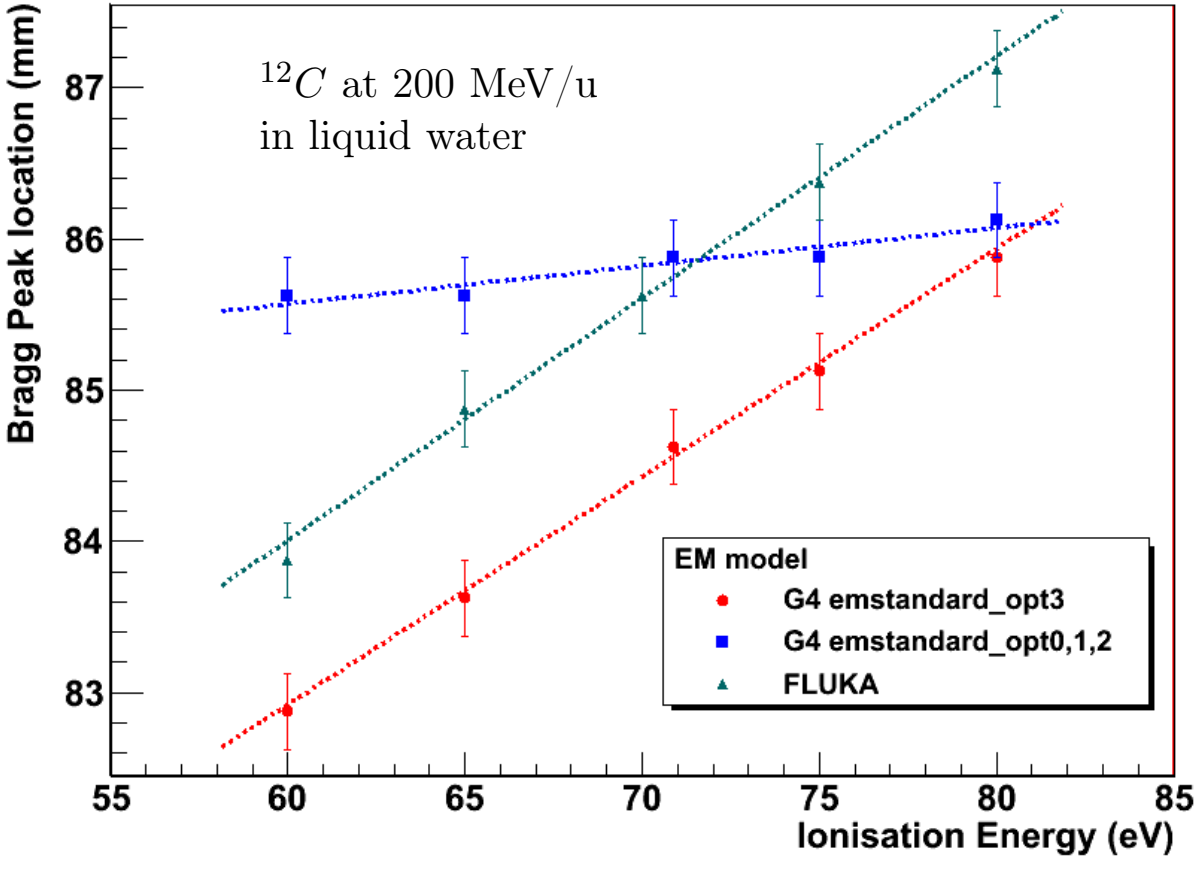

The Bragg Peak location depends on:

- the ionisation model
- the $< I >$ value
- $\Delta < I >= 5\,eV \longrightarrow \Delta range \approx 1\,mm$

Other processes

- elastic Coulomb scattering: trajectory is not a straight line (range and lateral spreading)
- elastic collision with target nuclei: contribution at $E_c < 10keV/u$ (few last μm). Neglected for hadrontherapy applications.
- electron capture at $E_c < 10MeV/u$ (close to the Bragg Peak), replace Z_p by $Z_{eff} = Z_p \left[1 - exp(-125\beta Z_p^{-2/3})\right]$ in the Bethe-Bloch equation
- Bremsstrahlung: neglected for hadrontherapy applications.
- Nuclear collisions: production of secondary particles
  big influence on the dose map

Stopping power

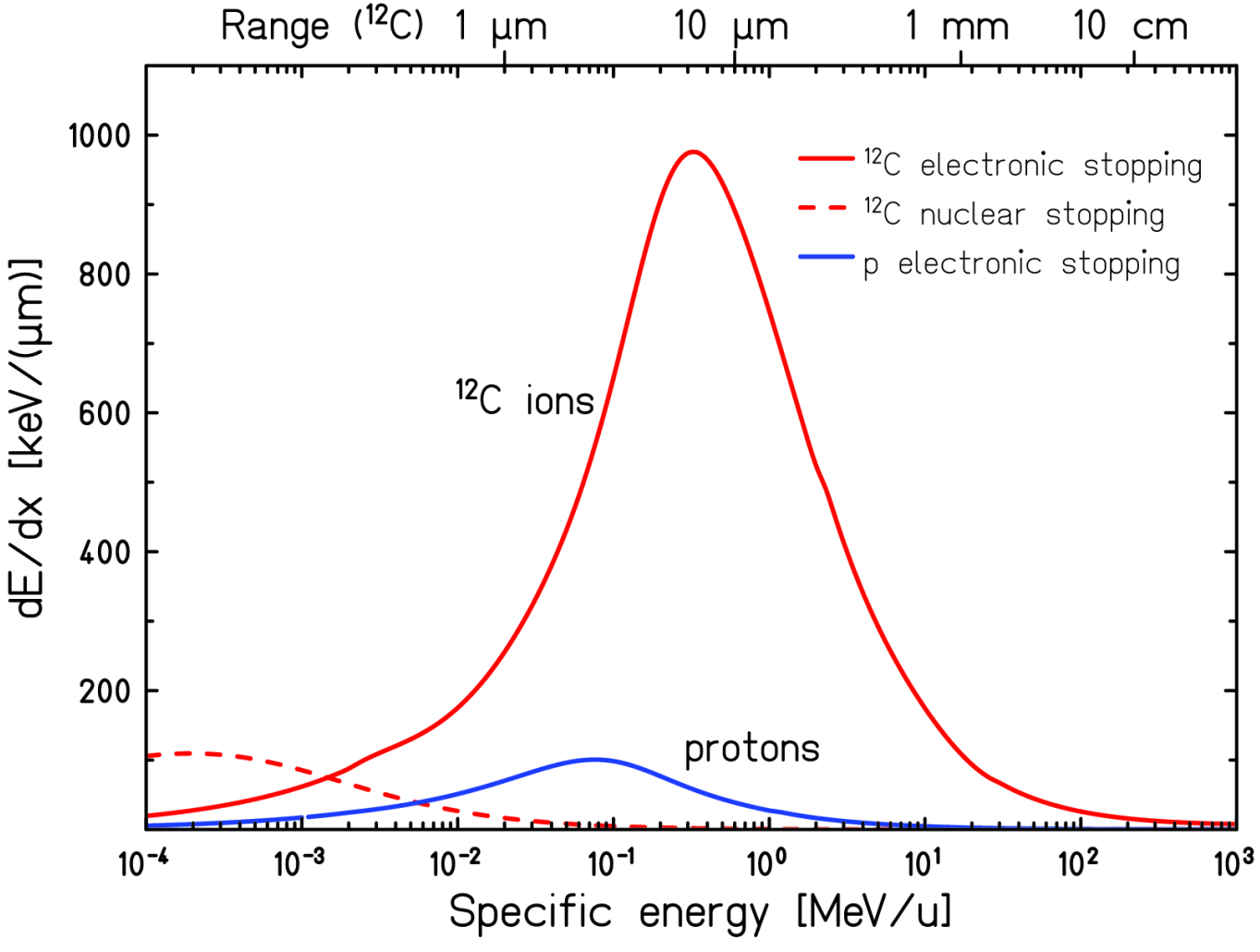

Particle range and particle energy

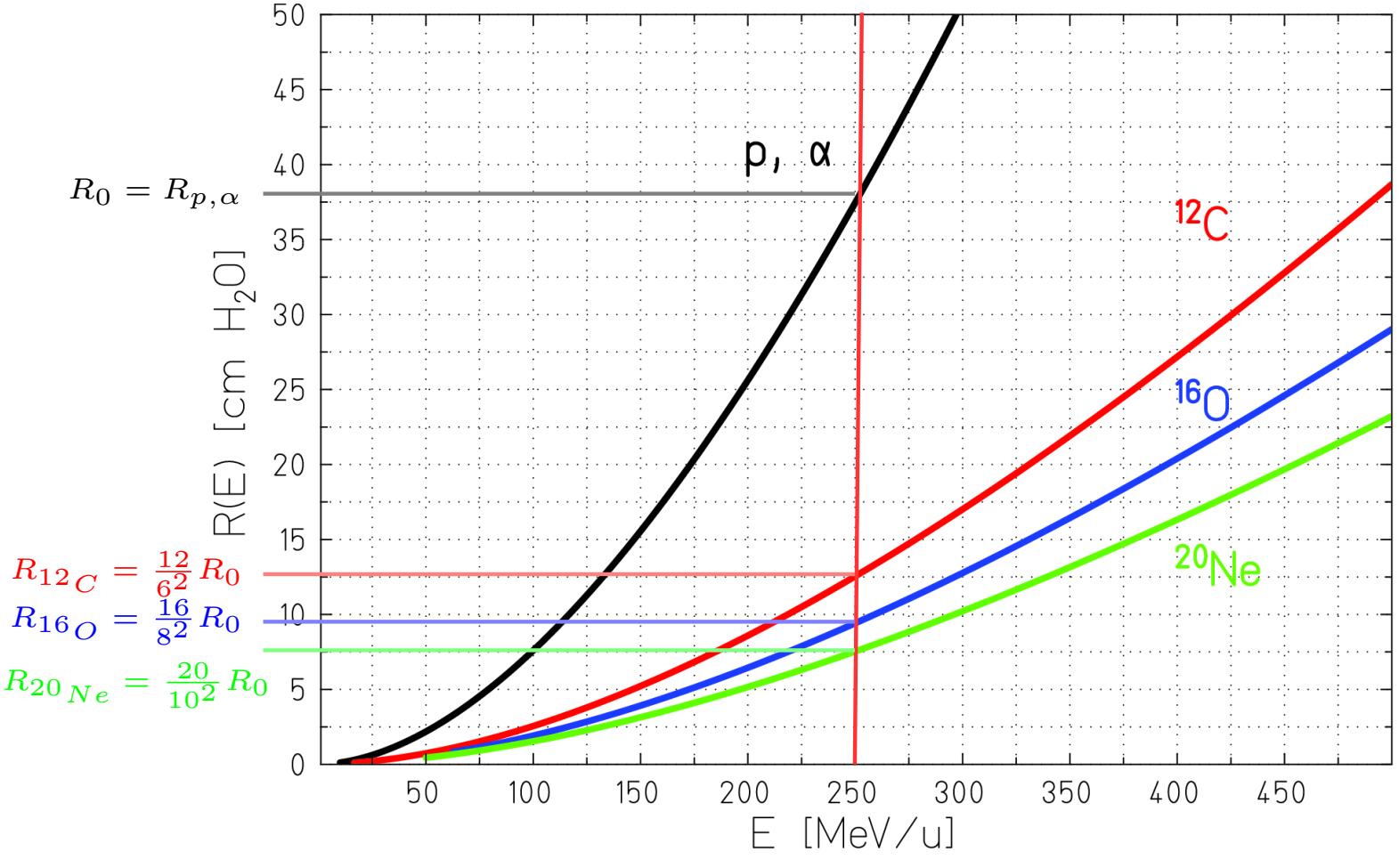

For a given energy, the range is proportional to $\frac{A}{Z^2}$

Particle range and particle energy

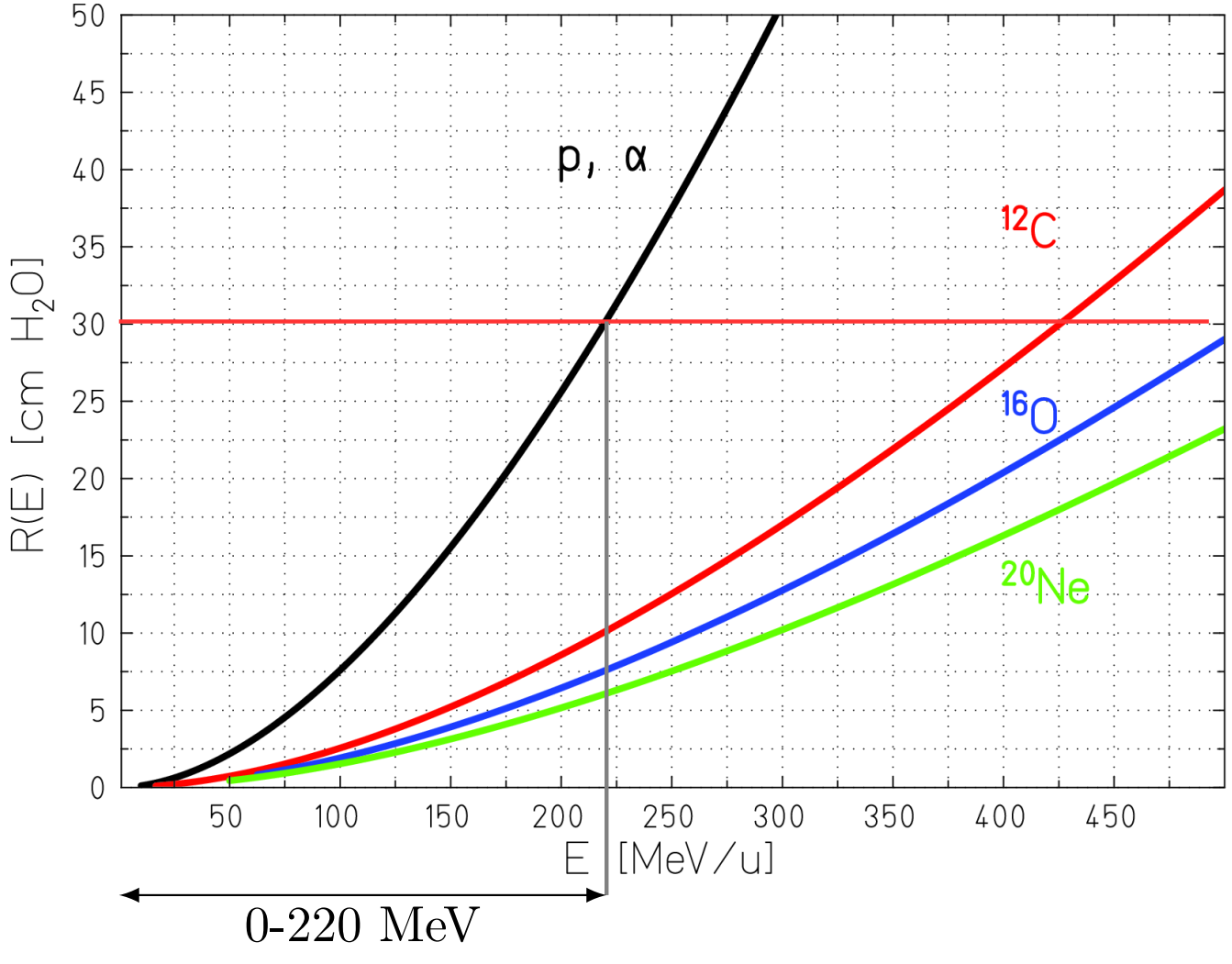

Particle range and particle energy

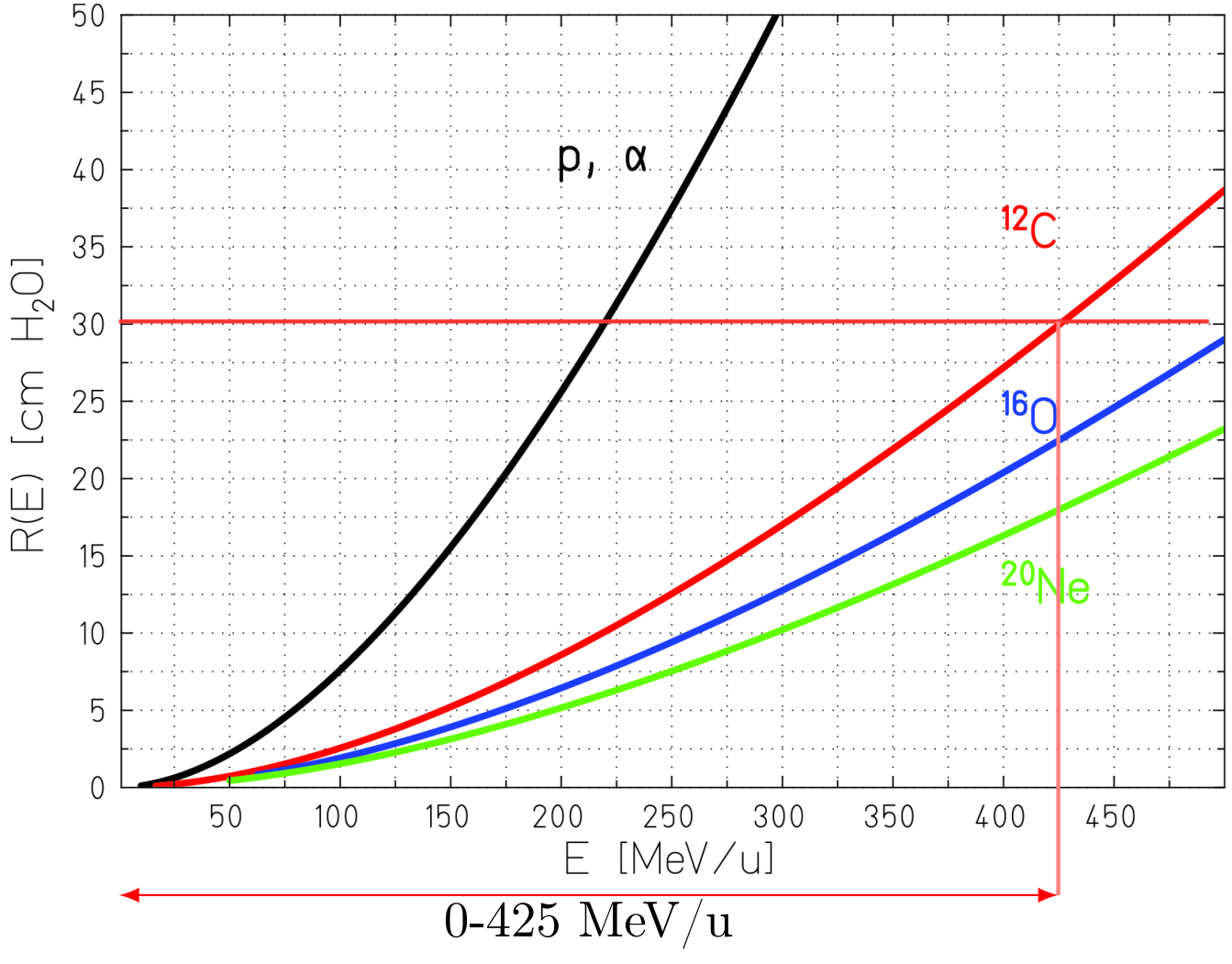

Range spreading

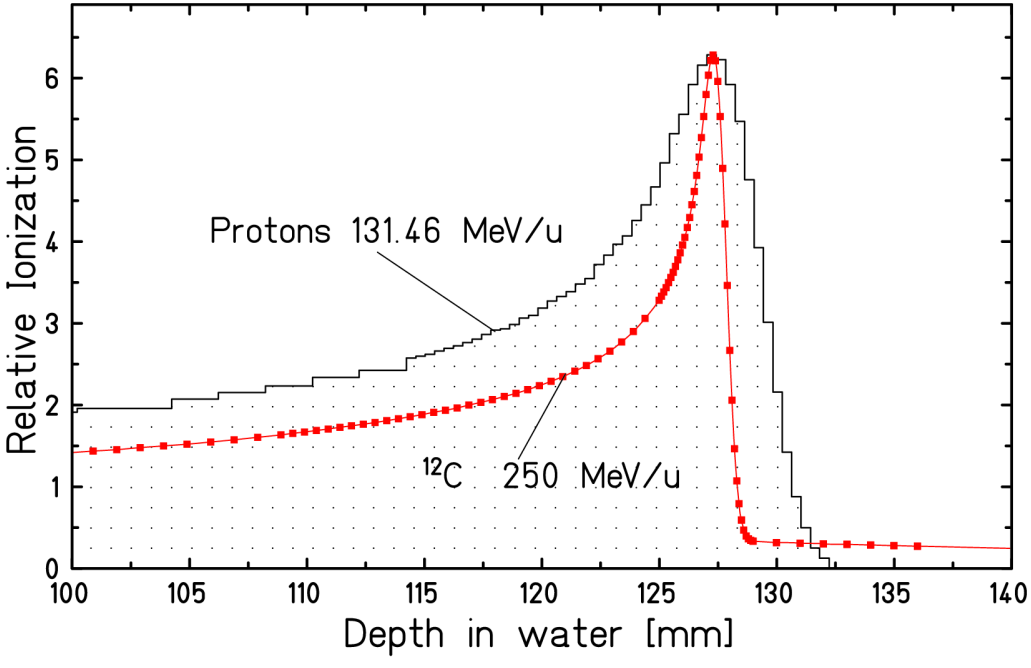

$$f(\Delta E) = \frac{1}{\sqrt{2\pi\sigma}} exp \frac{\left(\Delta E - \overline{\Delta E}\right)^2}{2\sigma^2}$$

$$\sigma = 4\pi\, Z_{eff}\, Z_t e^2 N \Delta x \left[\frac{1-\beta^2/2}{1-\beta^2}\right]$$

$$\sigma_R^2 = \int_0^{E_i} \left(\frac{d\sigma}{dx}\right) \left(\frac{dE}{dx}\right)^{-3} dE$$

$$\frac{\sigma_R}{R} = \frac{1}{\sqrt{M}} f\left(\frac{E}{Mc^2}\right)$$

The range spreading is smaller for the heavy ions.

Lateral spreading

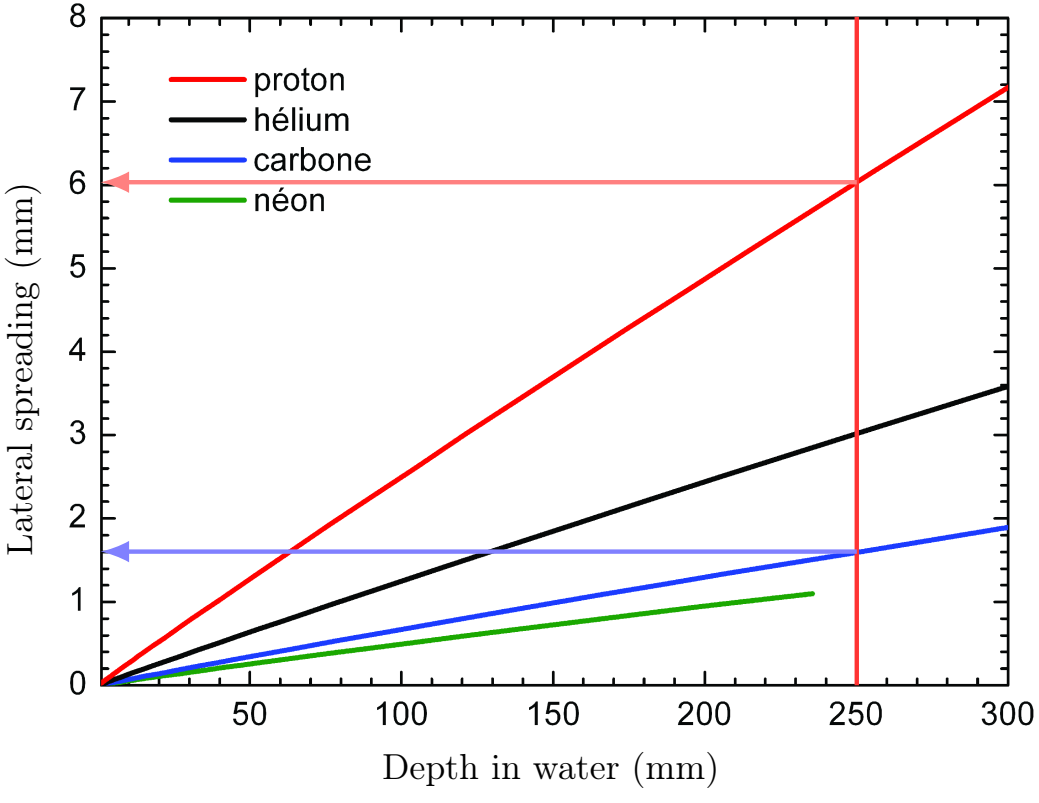

$$F(\vartheta, d) = \frac{1}{\sqrt{2\pi}\sigma_\vartheta} exp\left(-\frac{\vartheta^2}{2\sigma_\vartheta^2}\right)$$

$$\sigma_\vartheta[rad] = \frac{14.1MeV}{\beta pc} Z_p \sqrt{\frac{d}{L_{rad}}} \left[1 + \frac{1}{9} log_{10}\left(\frac{d}{L_{rad}}\right)\right]$$

SRIM calculations

The range spreading is smaller for the heavy ions.

Nucleus-Nucleus reactions

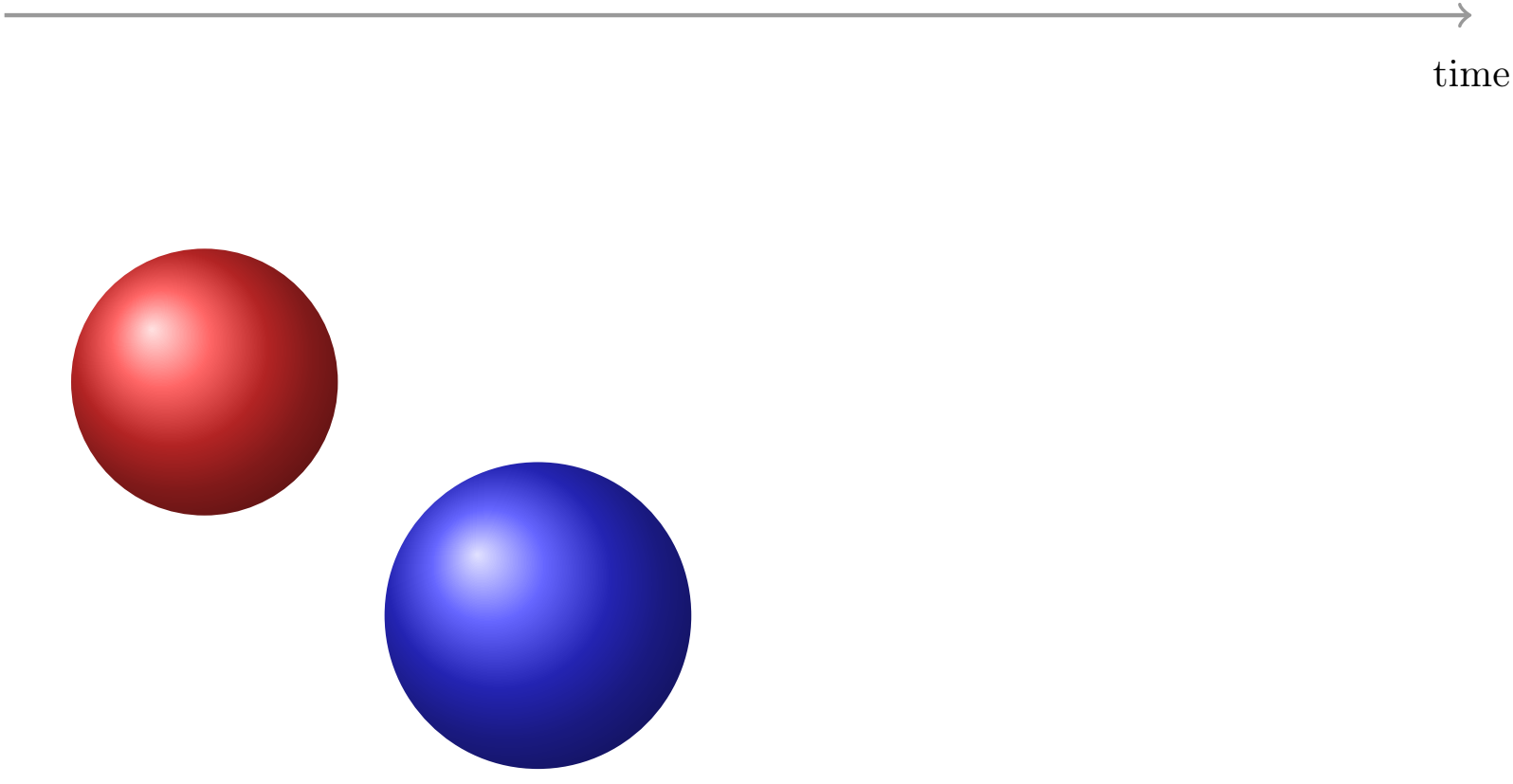

Nucleus-Nucleus reactions

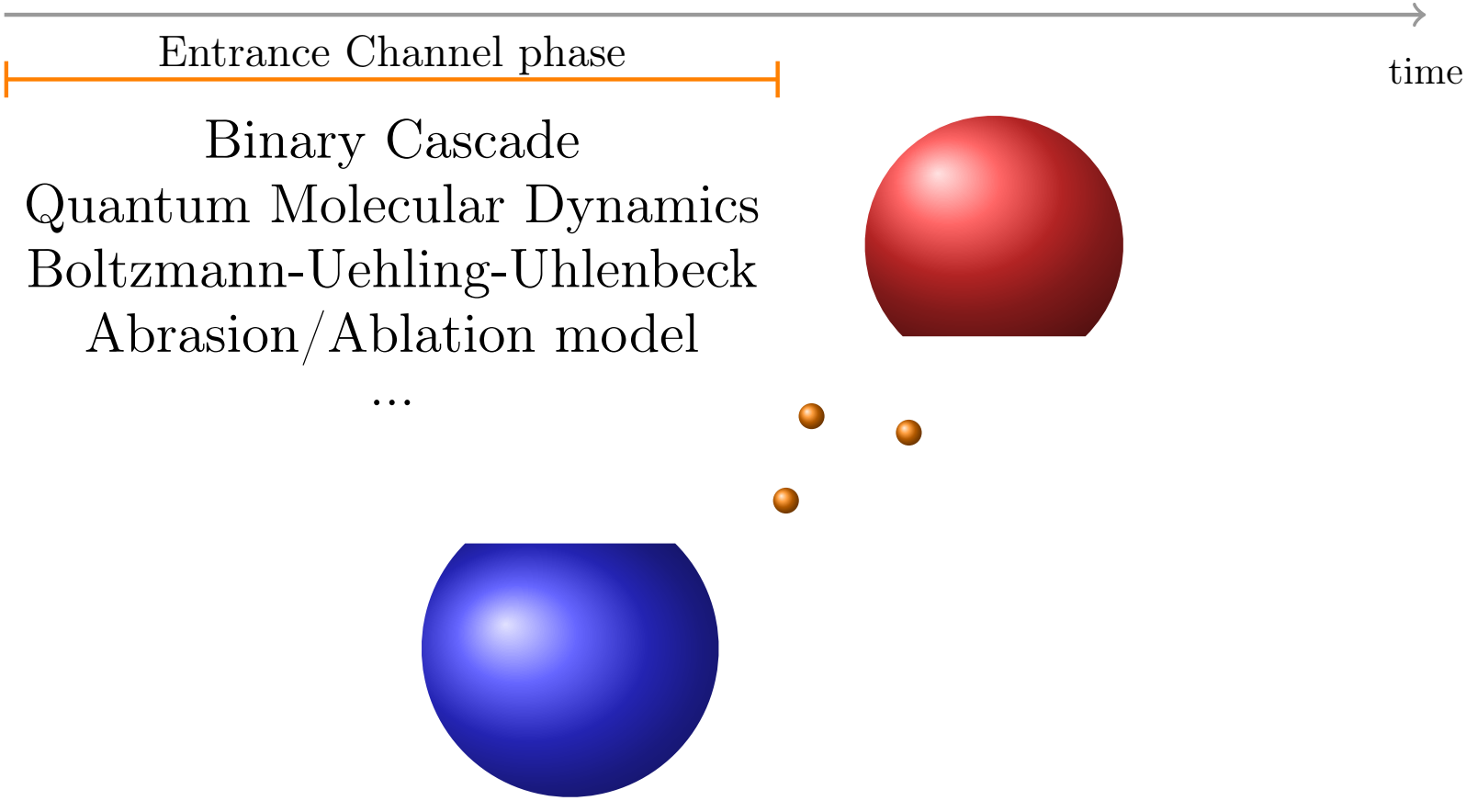

Nucleus-Nucleus reactions

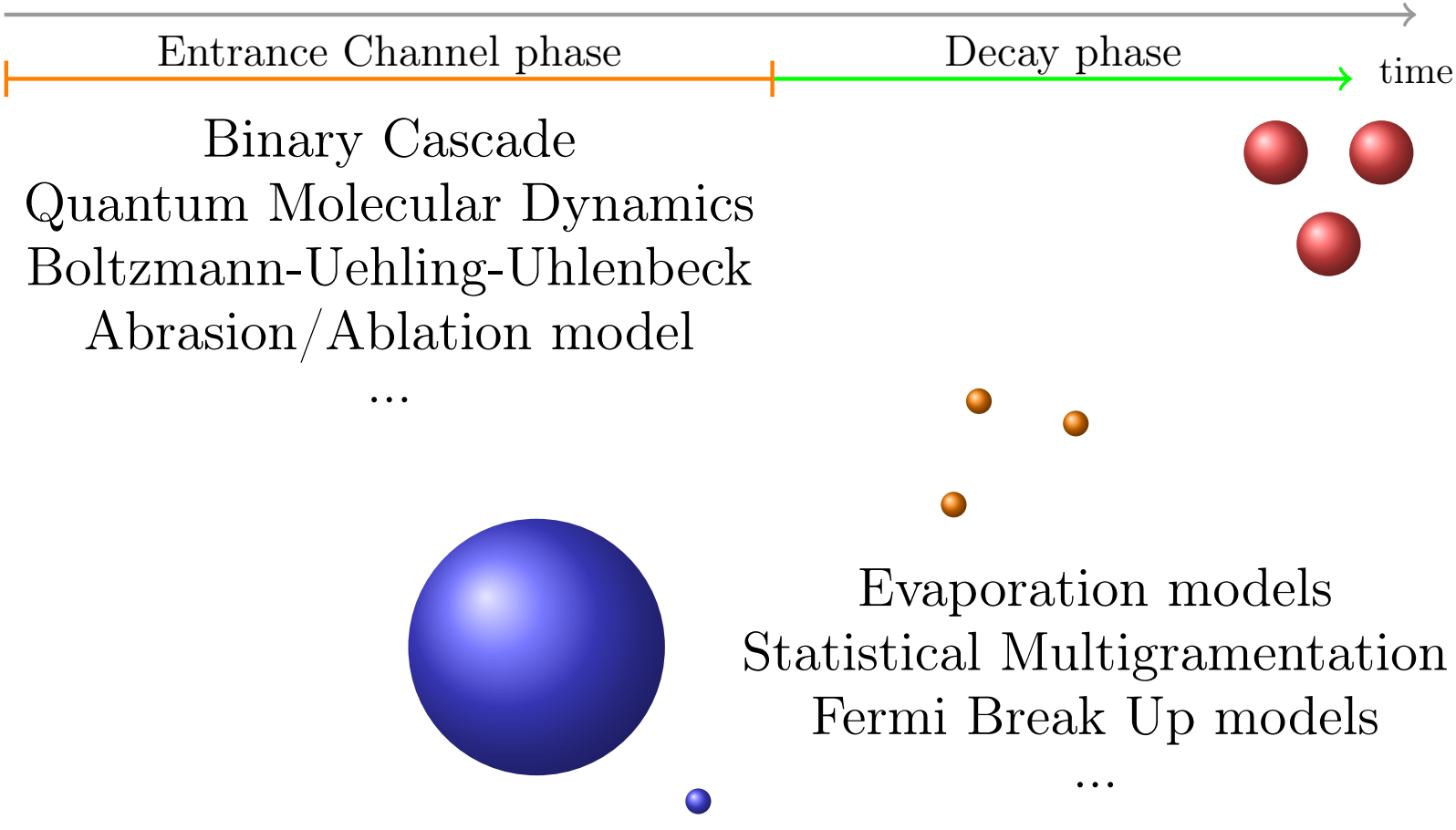

Contribution of secondary fragments

- the fragments emitted by the quasi-projectile have a velocity close to the projectile velocity and hence a longer range than the projectile range
- the fragments emitted by the quasi-target have a small velocity and have a very small range (few μm at most)
- the mid-velocity fragments have also a slightly longer range than the projectile range
- the most probable collisions are the peripheral collisions
  - $v_{QP} \lesssim v_{proj}$, $A_{QP} \approx A_{proj}$, $Z_{QP} \approx Z_{proj}$, E^*_{QP} small
  - $v_{fragments} \approx v_{QP}$
  - only very few mid-rapidity fragments

As a consequence

The dose delocalisation is mainly due to the fragments emitted by the quasi-projectile.

Energy balance

Energy conservation law

$$\Delta m_{A_p,Z_p}c^2 + T_{A_p,Z_p} + \Delta m_{A_t,Z_t}c^2 = \sum_i \left[\Delta m_{A_i,Z_i}c^2 + T_i\right]$$

$$\sum_i T_i = T_{A_p,Z_p} + Q$$

$$Q = \Delta m_{A_p,Z_p}c^2 + \Delta m_{A_t,Z_t}c^2 - \sum_i \Delta m_{A_i,Z_i}c^2$$

for the small systems ($Z < 26$), Q is negative $\Longrightarrow$ $\sum_i T_i < T_{A_p,Z_p}$

Example

$$^{12}C + ^{16}O \longrightarrow 3\,\alpha + ^{12}C + 2\,p + 2\,n$$

$$Q = \Delta m_{^{12}C}c^2 + \Delta m_{^{16}O}c^2 - 3\,\Delta m_{^4He}c^2 - \Delta m_{^{12}C}c^2 - 2\,\Delta m_{proton} - 2\,\Delta m_{neutron}$$

$$Q = 0.\,keV - 4737.05\,keV - 3 \times 2424.91\,keV - 0.\,keV - 2 \times 7289.03\,keV - 2 \times 8071.37\,keV = -42732.58\,keV$$

$\approx 42.7\,MeV$ are lost due to the nucleus-nucleus collision!

Effect on the Bragg curve for protons

GEANT4 simulations

$N(x) \approx N_0 e^{-x/\lambda}$

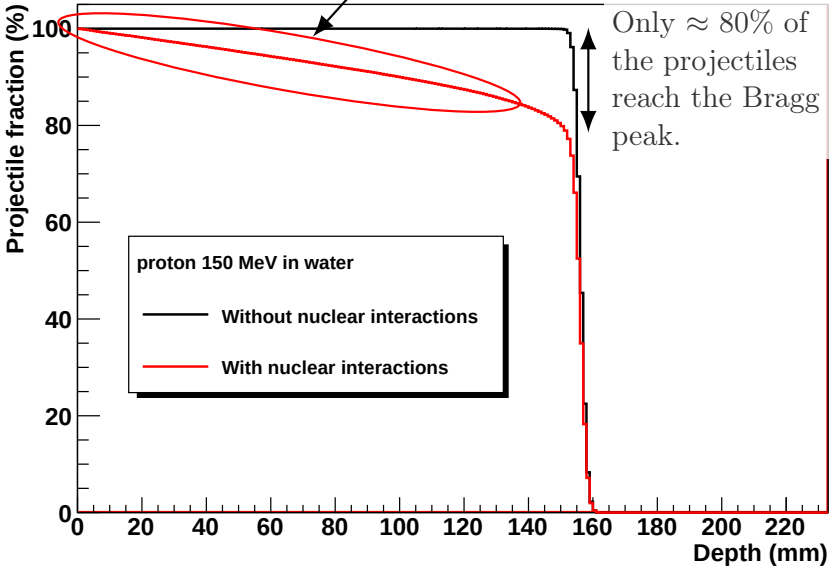

The Bragg Peak location is not modified

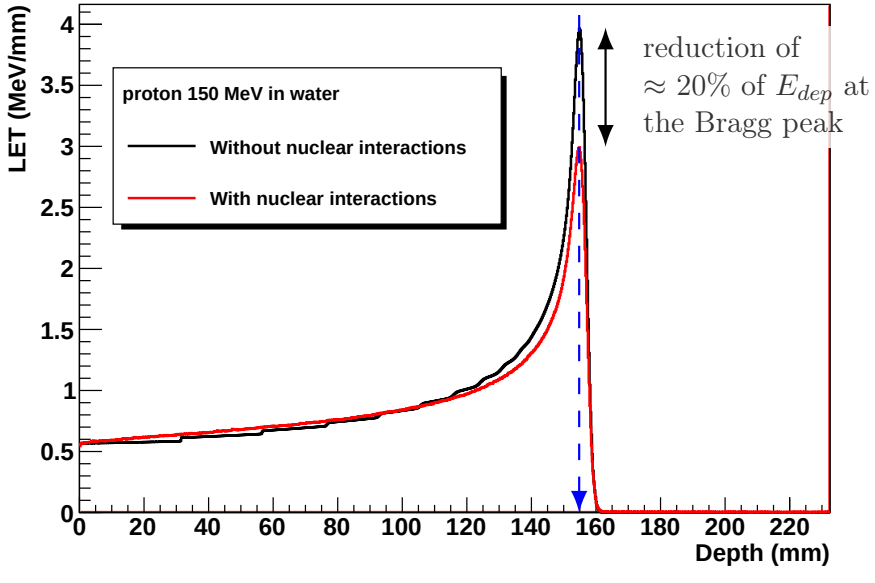

$\int LET(x)dx = E_{proj}$

$\int LET(x)dx = 0.97\ E_{proj}$

Effect on the Bragg curve for ^{12}C

GEANT4 simulations

$N(x) \approx N_0 e^{-x/\lambda}$

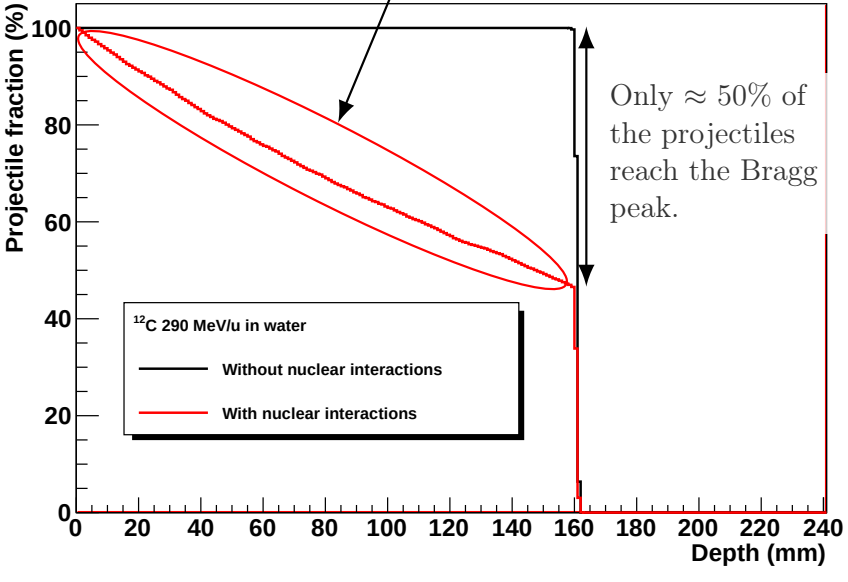

The Bragg Peak location is not modified

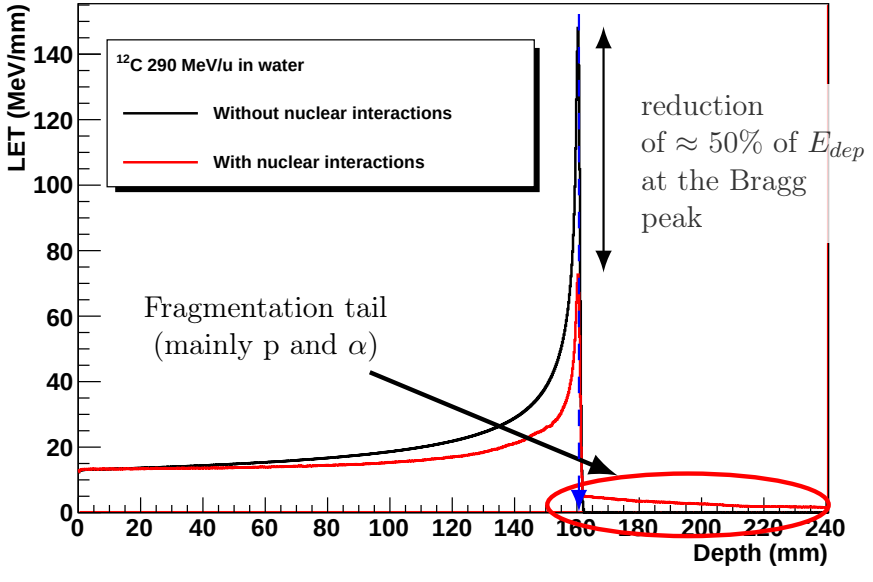

$$\int LET(x)dx = E_{proj}$$

$$\int LET(x)dx = 0.93\ E_{proj}$$

To summarize...

The nucleus-nucleus collisions:

- Do not change the location of the Bragg peak.
- Reduce the number of projectiles all along the path $N(x) \approx N_0 e^{-x/\lambda}$.
- Reduce the energy deposition at the Bragg peak $LET_{Nuc}(x_{BP}) \approx LET_{EM}(x_{BP}) e^{-x_{BP}/\lambda}$.
- Lead to an energy deposition beyond the Bragg peak: contribution of secondary particles.
- Reduces the total energy deposited in the target.

As a consequence

The dose map is significantly changed by the nucleus-nucleus collisions!

$N(x) \approx N_0\, e^{-x/\lambda}$

How many projectiles still remain after a path of length dx?

$$dN = -N\frac{N_t\,\sigma}{S} \qquad N_t = \frac{\mathcal{N}_a \rho S dx}{M_{mol}}$$

$$dN = -N\frac{\mathcal{N}_a \rho \sigma}{M_{mol}} dx$$

$$N(x) = N_0\, e^{-x/\lambda} \text{ with } \lambda = \frac{M_{mol}}{\mathcal{N}_a \rho \sigma}$$

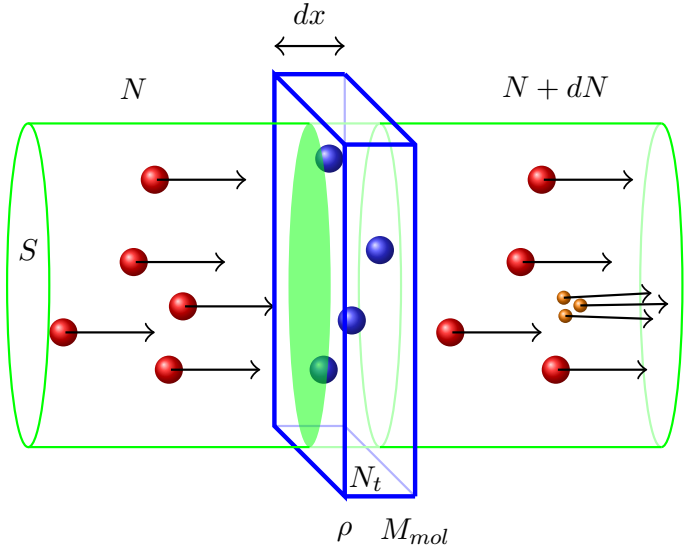

Consequences

- The reduction of the number of projectiles and the reduction of the LET value at the Bragg peak are directly linked to the nucleus-nucleus collision cross section σ
- The dose map depends on the chemical composition of the target material.

Numerical example

^{12}C at 290 MeV/u in water

$$\rho = 1\, g/cm^3,\ M_{mol} = 18\, g/mol,\ \mathcal{N}_a = 6.02\, 10^{23}$$

$$\sigma_{C,H} \approx 0.2\, b\ (= 2\, 10^{-25}\ cm^2)$$

$$\sigma_{C,O} \approx 1\, b\ (= 10^{-24}\, cm^2)$$

$$\sigma_{C,H_2O} = 2\, \sigma_{C,H} + \sigma_{C,O} \approx 1.4\, b$$

$$\lambda \approx \frac{18.}{6.02\, 10^{23}\, 1.\, 1.4\, 10^{-24}} \approx 21.35\, cm$$

for a ^{12}C at 290 MeV/u, $x_{BP} = 16\, cm$:

$$N(x_{BP}) \approx N_0\, e^{-16/21.35} \approx 0.47\, N_0$$

Influence of the nucleus-nucleus collision cross section

GEANT4 simulations

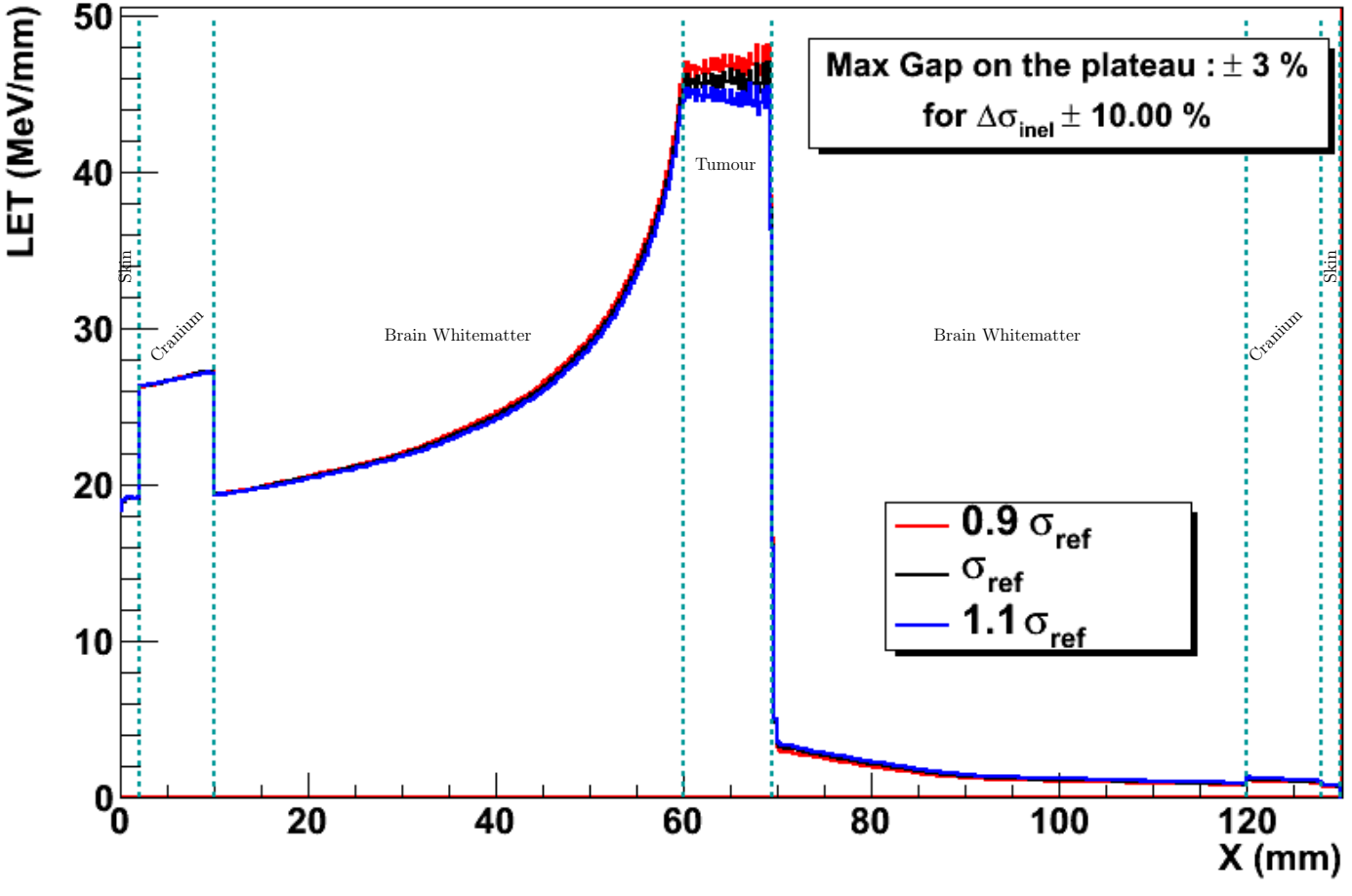

Secondary particles multiplicities

Experimental data (GSI)

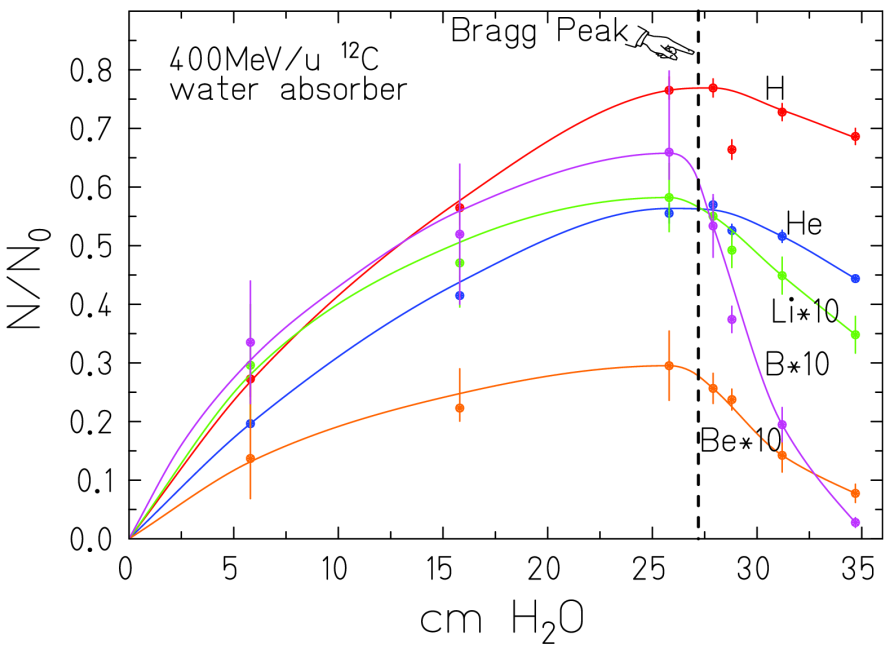

E.Haettner, H. Iwase, and D. Schardt, Radiat. Prot. Dosim. 122 (2006) 485–487

GEANT4 simulation

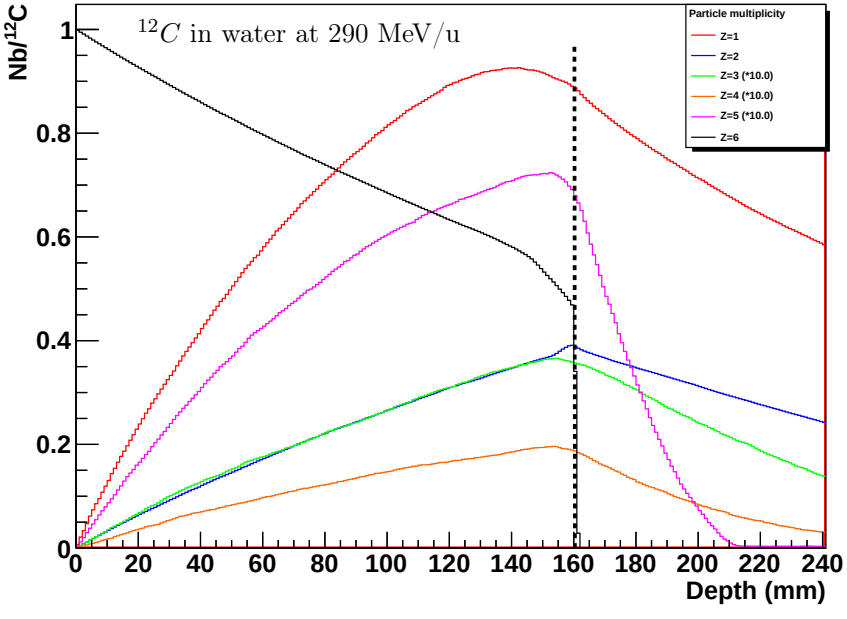

Secondary particles LET

GEANT4 simulations

^{12}C in water at 290 MeV/u

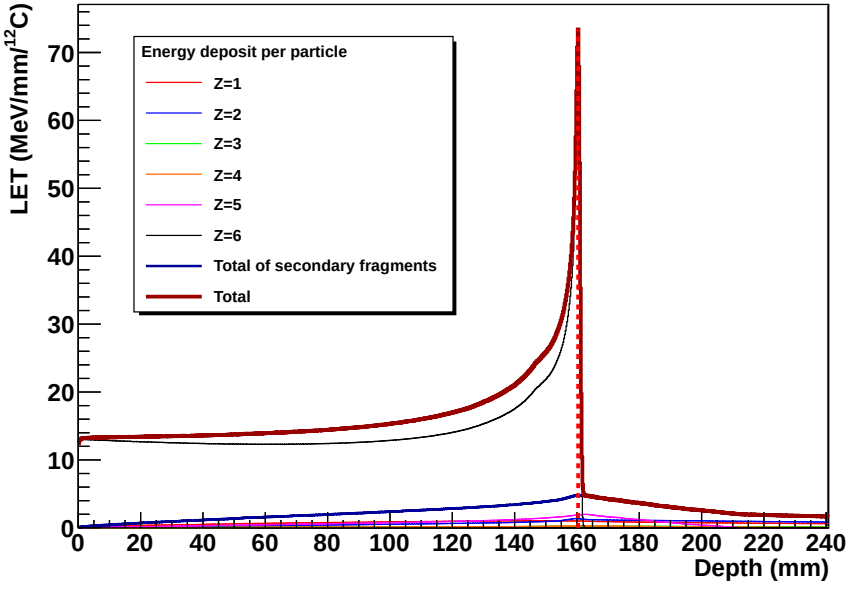

zoom on low LET values

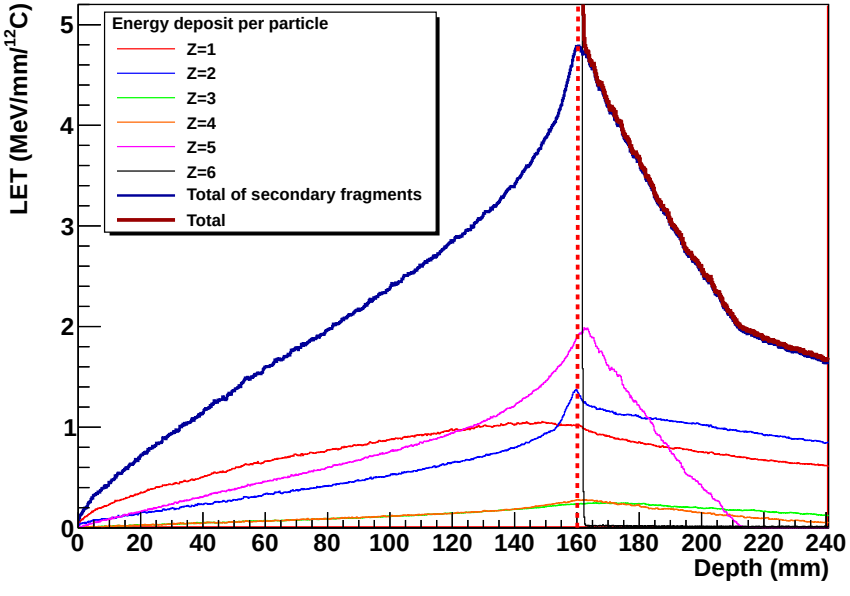

The contribution of secondary particles is ≈ 7 % at the Bragg Peak

The nucleus-nucleus collision models in GEANT4

The entrance channel models in GEANT4

- Binary Cascade (BIC)
- Quantum Molecular Dynamics (QMD)

The decay models in GEANT4

- Evaporation model (EVAP) or Generalized Evaporation Model (GEM) for all nuclei.
- Fermi Break Up (FPU) for $4 < A < 17$ and $Z < 9$.
- Statistical Multiframentation Model (MF) for $A > 5$ and $E^*/A > 3\,MeV$.

The decay models can be used simultaneously in GEANT4 for the first decay of the excited nucleus. The secondary decays are always done through the evaporation model.

The BIC model in GEANT4

J.Cugnon, C. Volant and S. Vuillier, Nuc. Phys. A 620 (1997) 475-509

G. Folger, V.N. Ivanchenko, and J. P. Wellisch, Eur. Phys. Jour. A 21, 407-417 (2004)

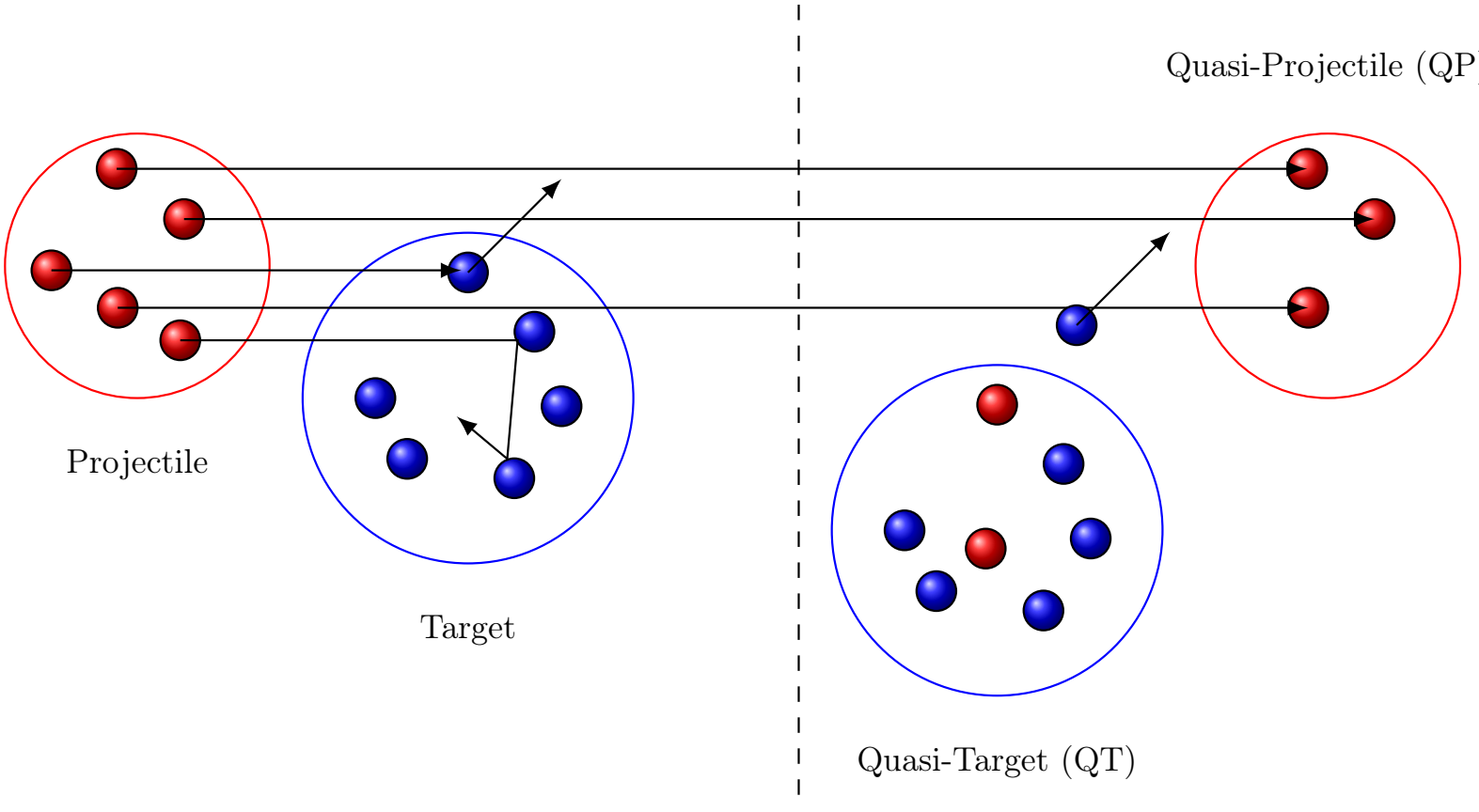

The QMD model in GEANT4

$$f(\vec{r},\vec{p},t) = \sum_i \left[\lambda_i e^{-\frac{(\vec{r}-\vec{r_i})^2}{2\sigma_r^2} - \frac{(\vec{p}-\vec{p_i})^2)}{2\sigma_p^2}} \right]$$

$$\frac{\partial f}{\partial t} + \frac{\vec{p}}{m}\vec{\nabla}_r f - \vec{\nabla}_r U \vec{\nabla}_p f = I_{collision}(f)$$

for QMD, 1 gaussian per nucleon is used to sample the one-body distribution function $f(\vec{r},\vec{p},t)$. *K. Niita et al. Phys. Rev. C 52, 2620-2635 (1995)*

Ni + Au, 7 MeV/u, b=4 fm

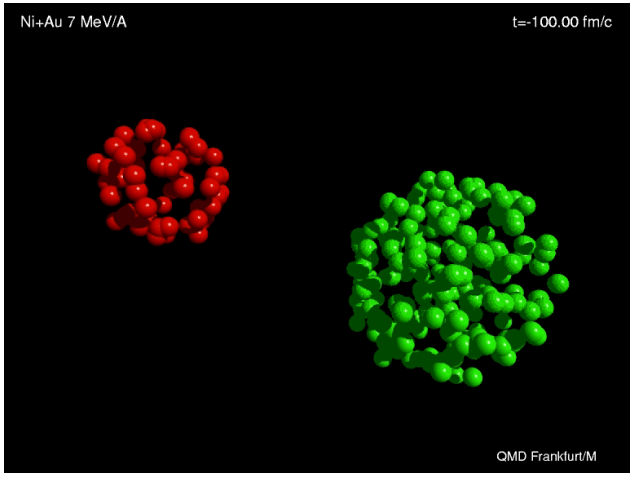

Statistical decay models

The basis

- For each decay configuration $\{Z_i, A_i\}$ a weight $\mathcal{W}(E^*, J, \{Z_i, A_i\})$ is computed.
- The decay configuration is chosen according to its statistical weight $\mathcal{P}(\{Z_i, A_i\}) = \mathcal{W}(E^*, J, \{Z_i, A_i\}) / \sum_{configurations} \mathcal{W}(E^*, J, \{Z_j, A_j\})$
- Different statistical ensembles (microcanonical, canonical, grand canonical) or formalisms may be used to compute the configurations weights.

The evaporation models

- The configurations with two particles only are taken into account.
- EVAP model: only the emissions of light particles $(n, p, d, t, {}^3He, \alpha)$ are considered.
- Generalized Evaporation Model: all the configurations with two particles are considered.

The fragmentations models

- No limitations on the particles multiplicity.
- Fermi Break Up models: all the possible partitions are considered.
- Statitical Multifragmentation Model: a reduced sample of configurations is randomly chosen among all the possible configurations.

Influence of the model for ^{12}C

GEANT4 simulations

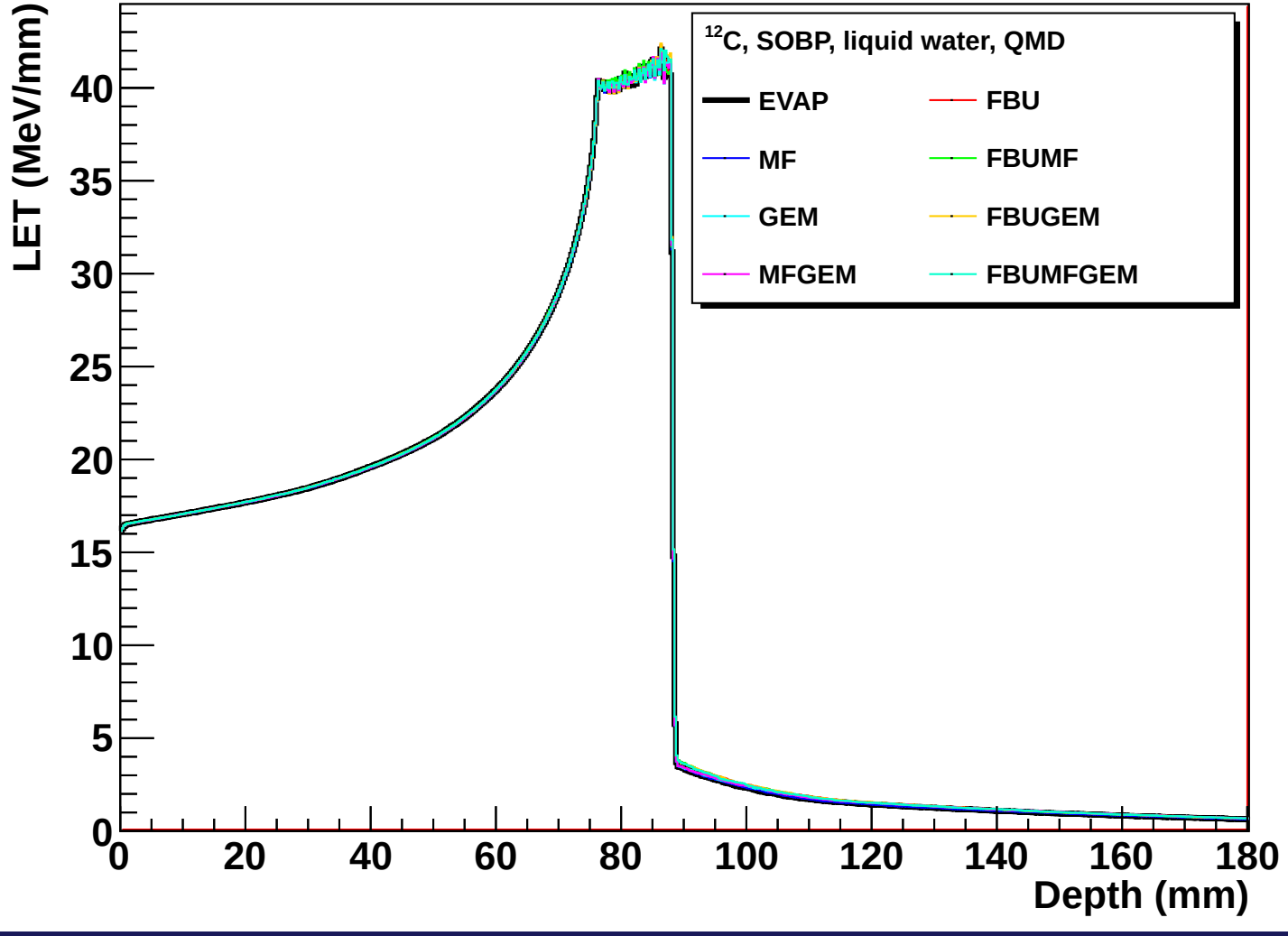

Comparison of Bragg Curves: Relative Gap

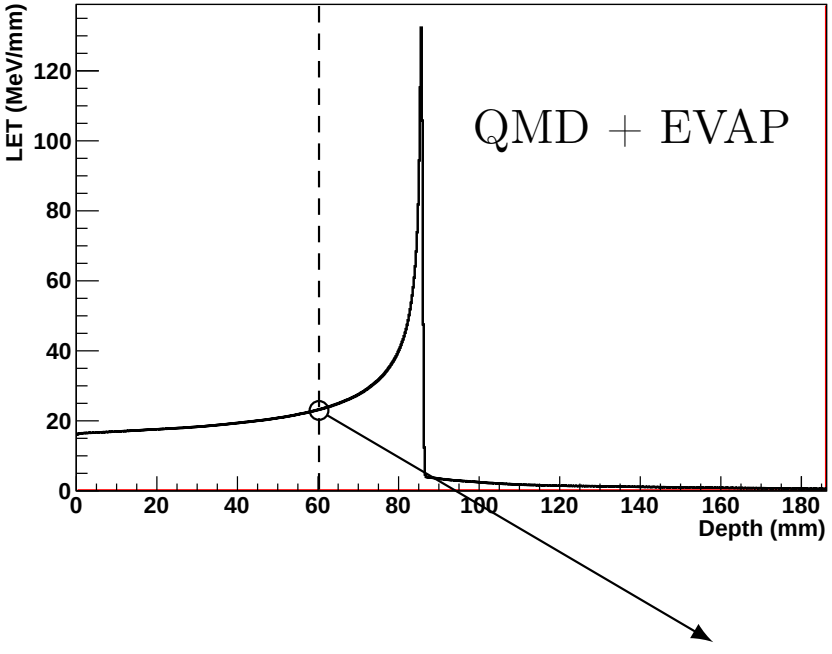

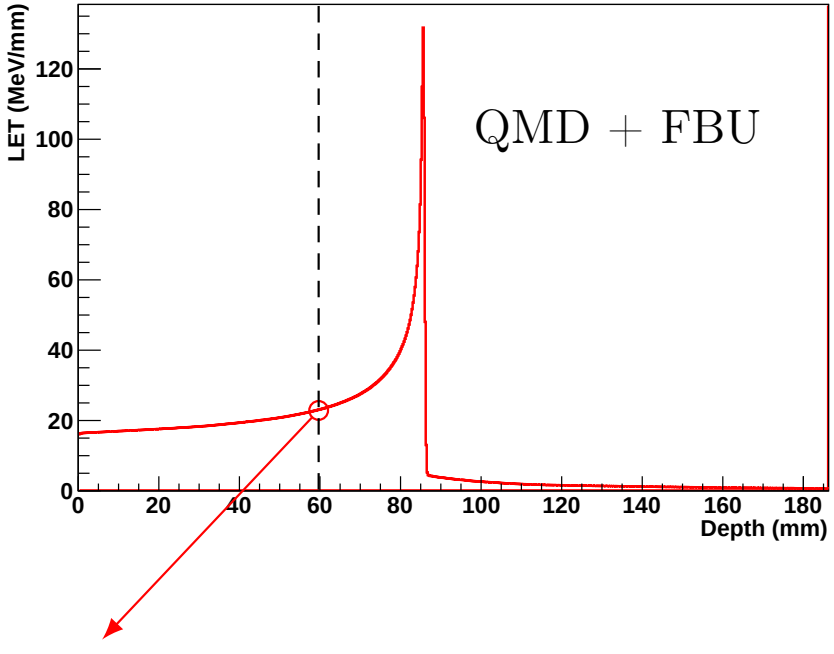

$$R(x) = \frac{Curve_1(x) - Curve_2(x)}{Curve_1(x)} \times 100$$

Influence of the decay model for ^{12}C

GEANT4 simulations

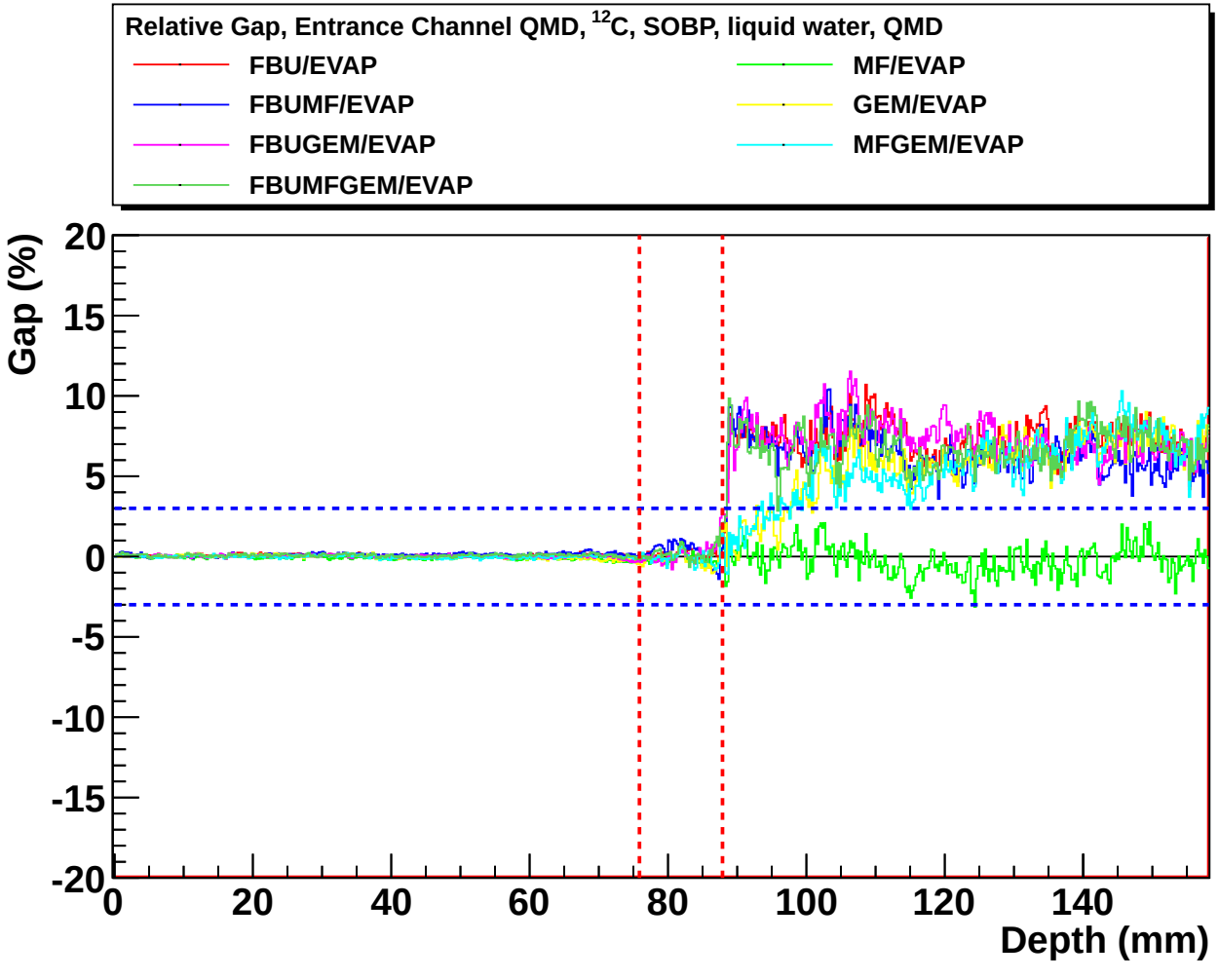

Influence of the entrance channel model for ^{12}C

GEANT4 simulations

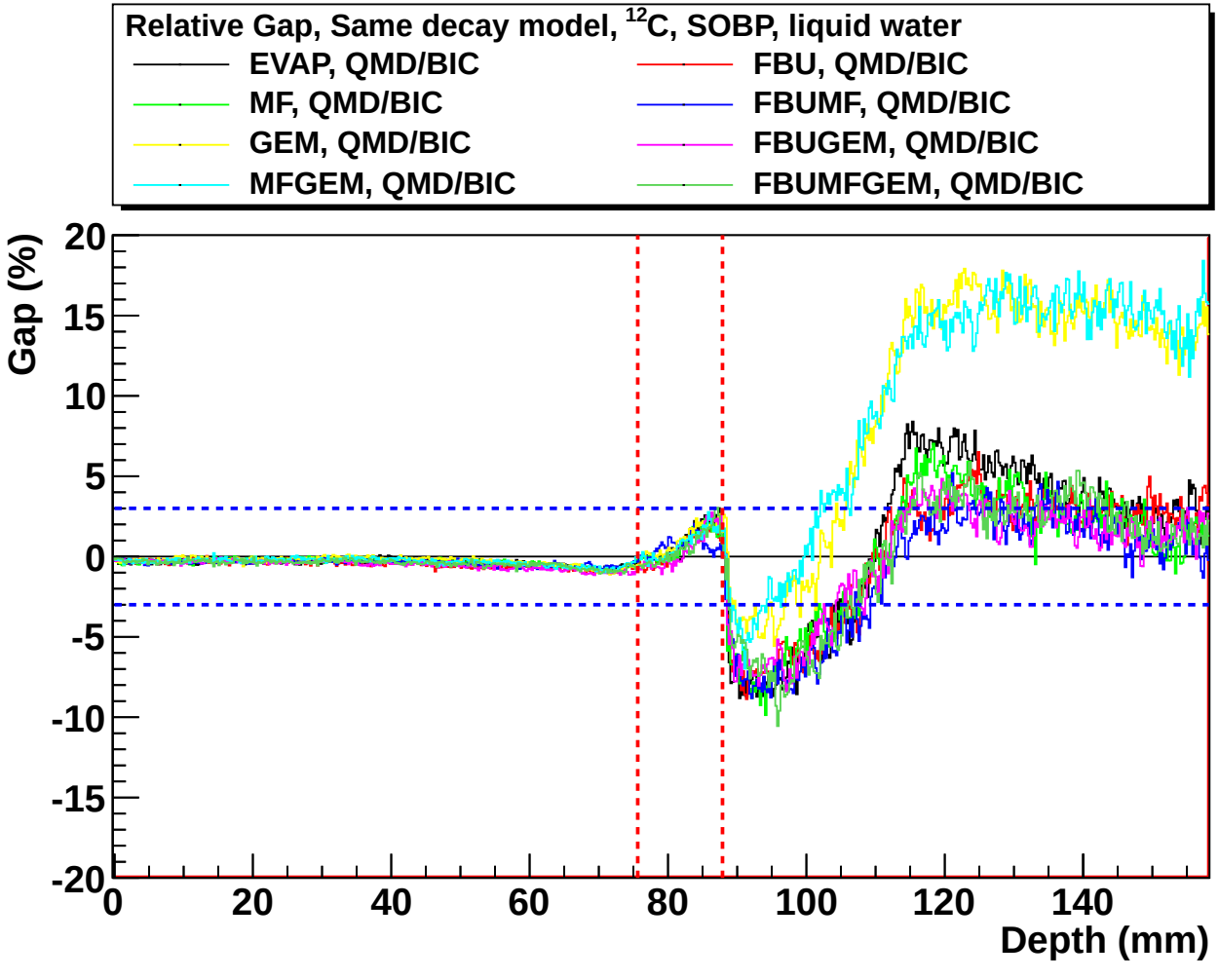

Influence of the collision model for ^{12}C: Summary

Decay model effect

- before the Bragg Peak: the relative gap is smaller than $\lesssim 0.5\%$
- after the Bragg Peak: the relative gap can reach $\approx 15\%$ but the doses are small

Entrance channel model effect

- before the Bragg Peak: the relative gap is smaller than $\lesssim 0.5\%$
- close to the Bragg Peak: the relative gap can reach $\approx 3\%$
- after the Bragg Peak: the relative gap can reach $\approx 20\%$ but the doses are small

As a consequence...

- the influence of the collision model on the dose is small ($\lesssim 3\%$)
- greater influence of the entrance channel
- big influence of the collision model if one wants tu use the secondary particles to monitor the dose!

Fragmentation experiments

E600 experiment at Ganil (IPN Lyon, IPHC Stasbourg, LPC Caen)

^{12}C at 95 MeV/u on thick PMMA targets

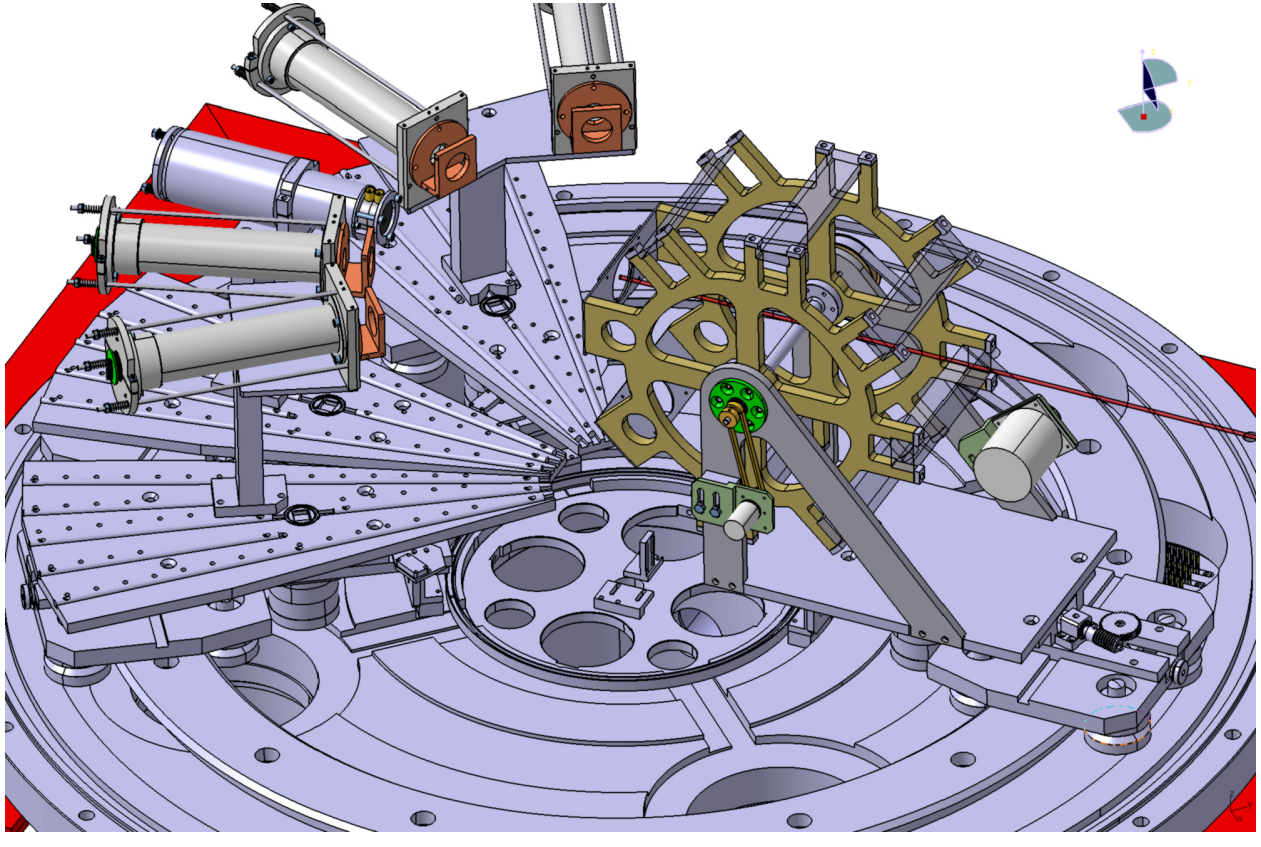

Fragmentation experiments (continued)

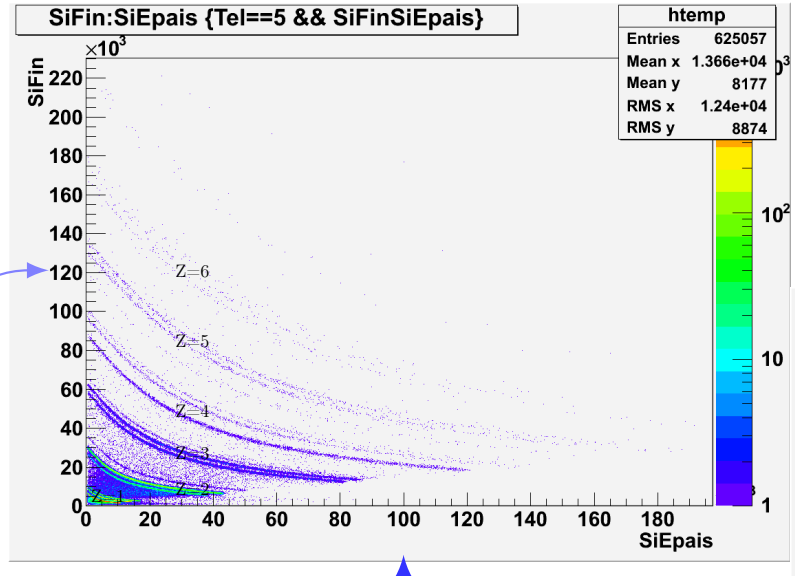

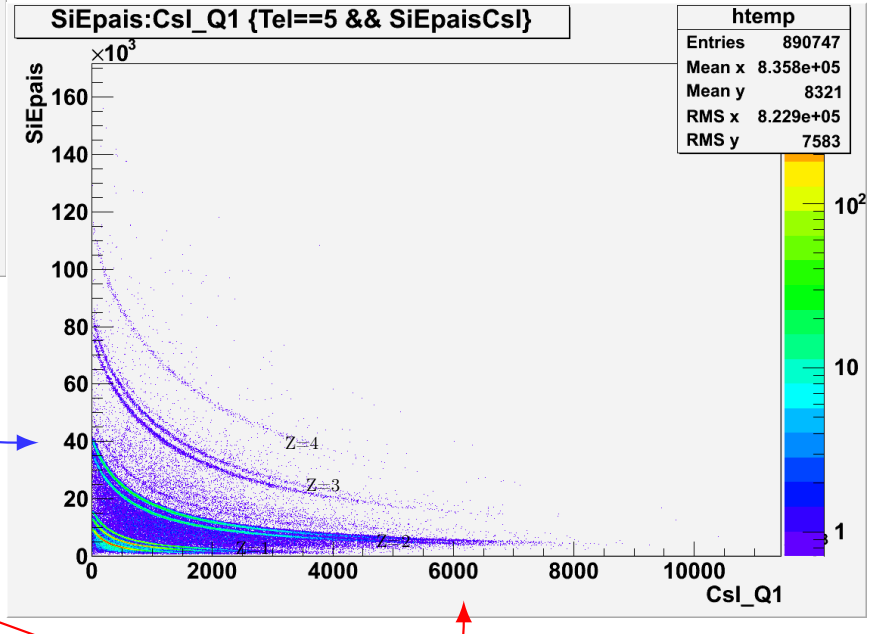

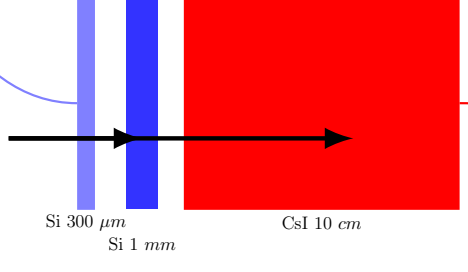

Fragmentation experiments (results)

^{12}C at 95 MeV/u (GANIL)

PMMA 25 mm, $\vartheta = 0°$

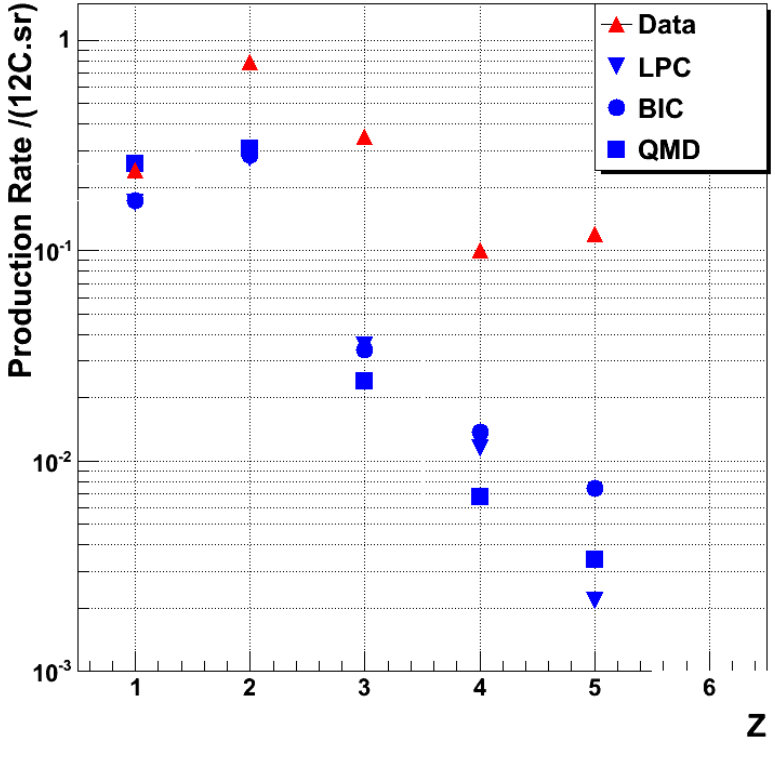

PMMA 5 mm, $\vartheta = 7°$

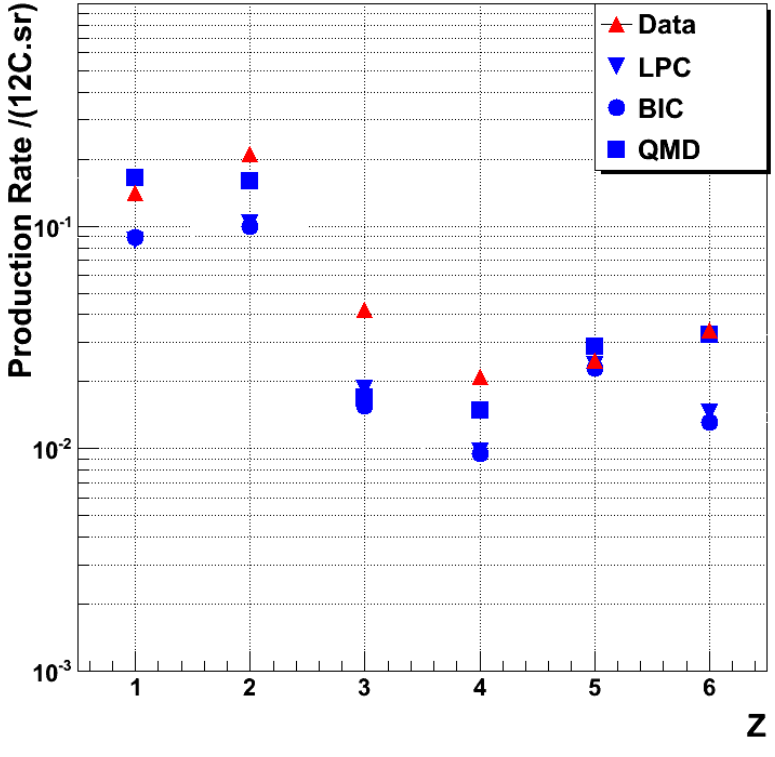

Benjamin Braunn PhD thesis

Treatment constraints for a clinical dose control

For a typical treatment

- The irradiation lasts 2 minutes at most
- The dose delivered per fraction is 2 Gy
- the total duration of an irradiation fraction is 20 minutes (positioning + irradiation)

To be efficient a control has to:

- use a process which produces enough statistics within the 2 Gy constraint
- have detectors with the best possible efficiency
- have a fast electronics and computer processing
- leave enough room for the patient, the positionning control devices, the irradiation table, ...

Dose control by using β^+ emitters

PMMA Target

protons at 140 MeV

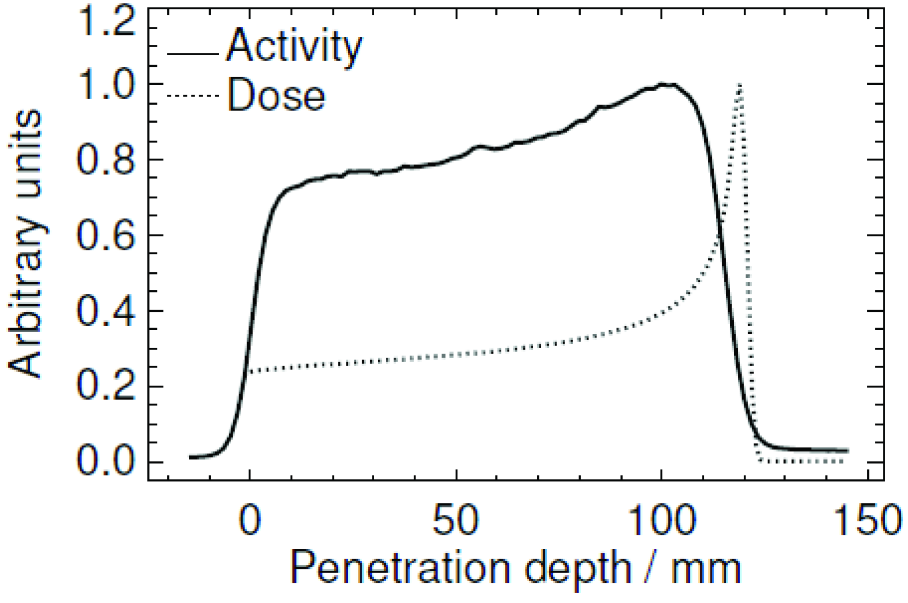

^{12}C at 259.5 MeV/u

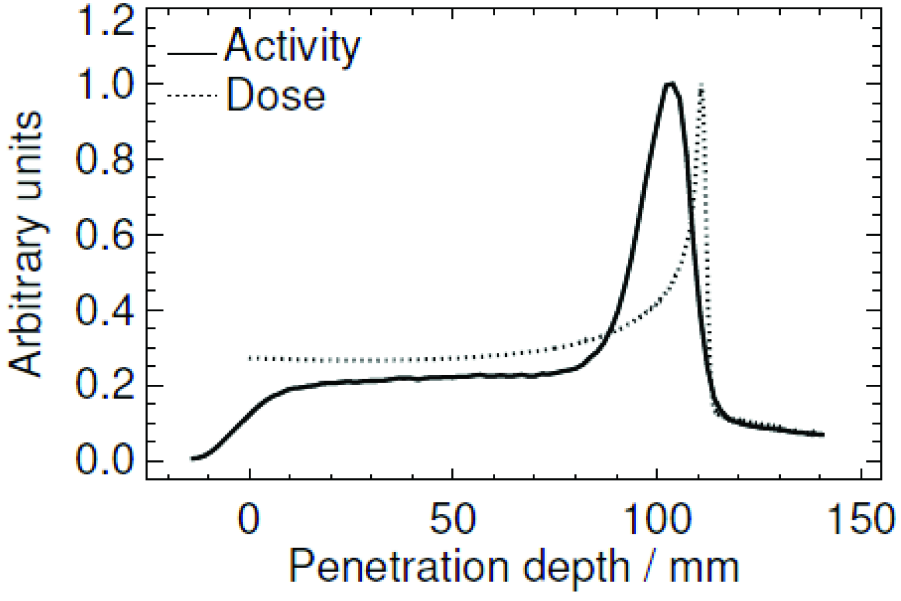

The main β^+ emitters are $^{11}C(T_{1/2} = 20.3\,mn)$, $^{10}C(T_{1/2} = 19.3\,s)$ and $^{15}O(T_{1/2} = 121.8\,s)$.

K. Parodi Ph.D. thesis (2004) Technische Universität Dresden, Fakultät Mathematik und Naturwissenschaften

Dose control by using β^+ emitters (continued)

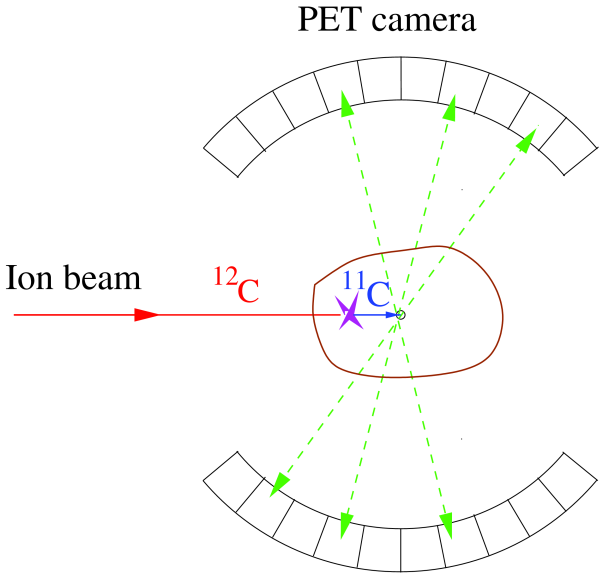

The PET camera at GSI

K. Parodi et al, Nucl. Instrum. Methods Phys. Res. A 591 (2008) 282–286.

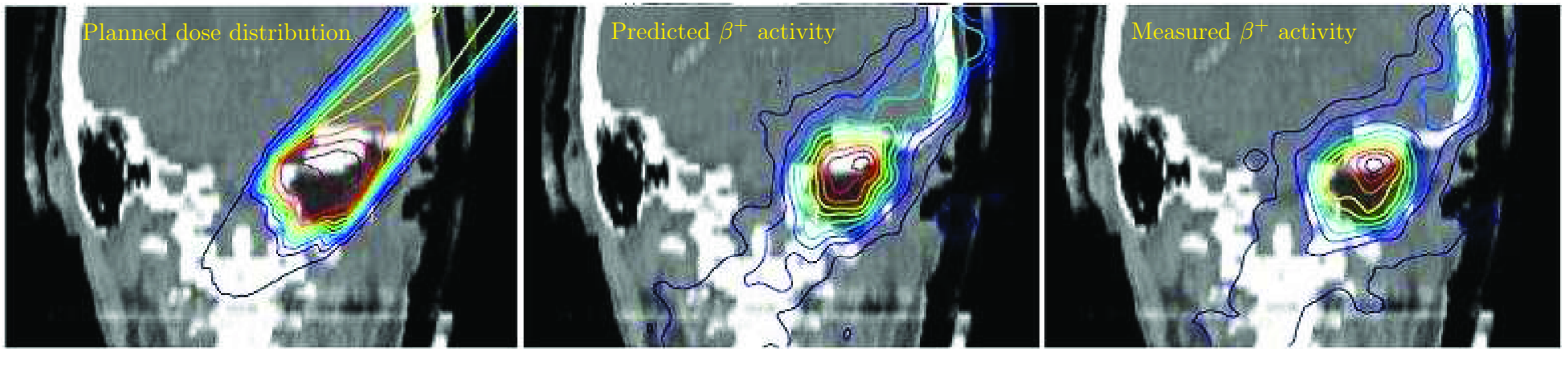

Enghardt, W., P. Crespo et al., Nucl. Instrum. Methods Phys. Res. A 525 (2004) 284–288.

Dose control by using prompt γ emissions

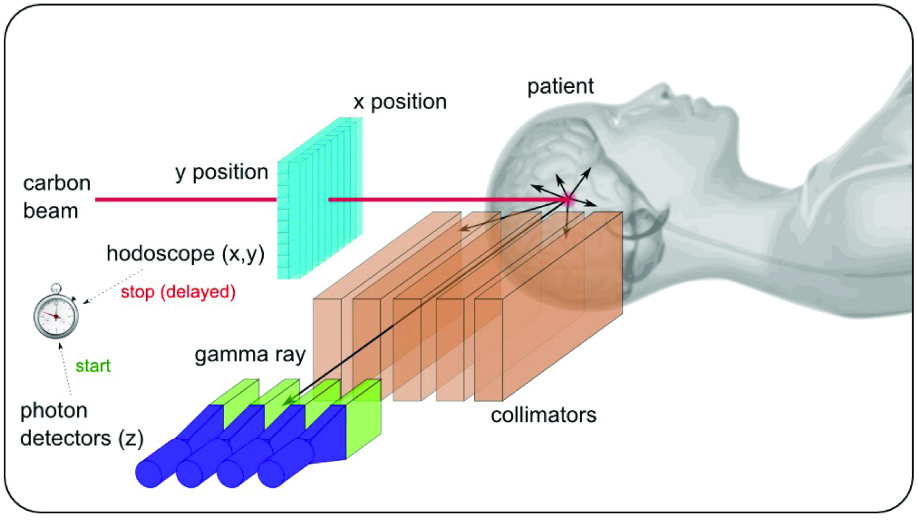

Collimated γ camera

F. Le Fouhler PhD thesis, 2010, Université Claude Bernard Lyon 1

Compton γ camera

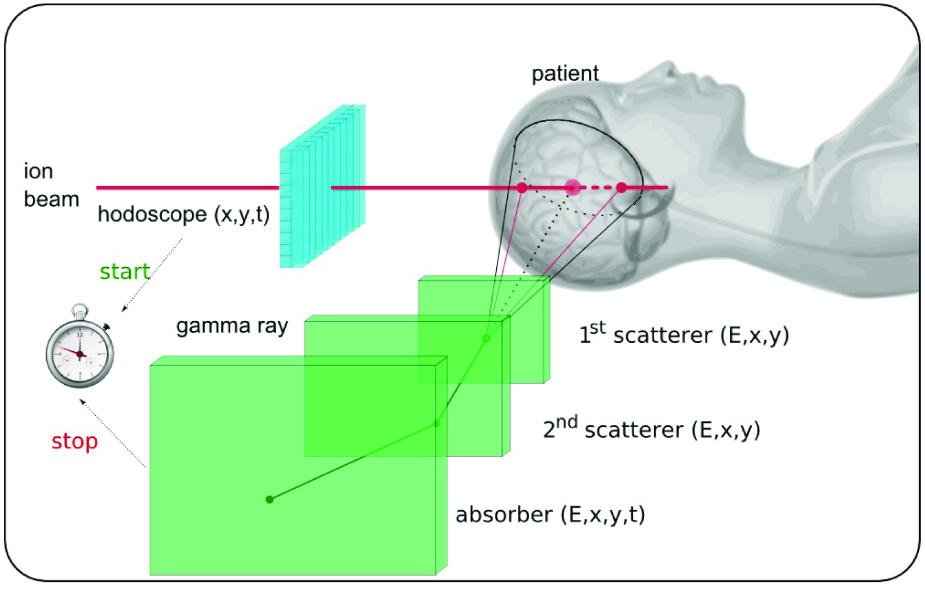

Dose control by using prompt γ emissions (continued)

PMMA thick target

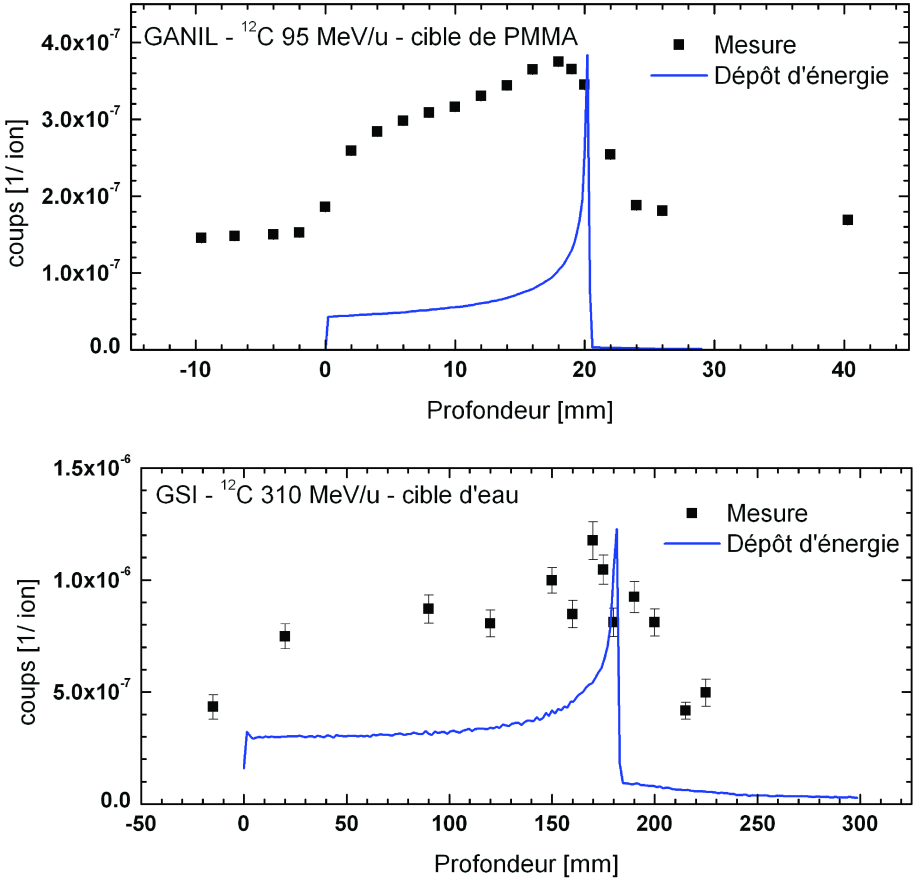

GEANT4 simulations, QMD+FBU

^{12}C at 310 MeV/u

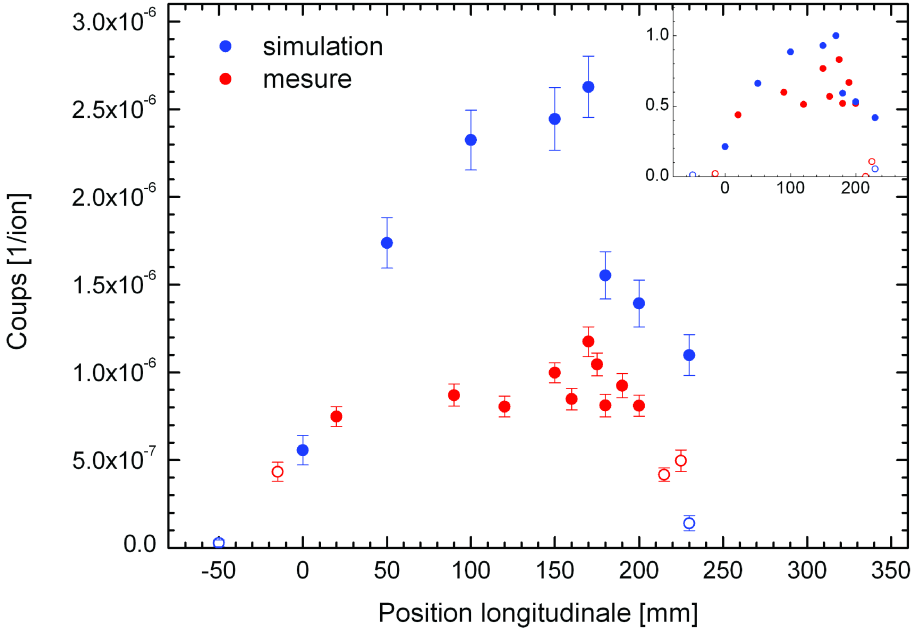

F. Le Fouhler PhD thesis, 2010, Université Claude Bernard Lyon 1

Dose control by using secondary charged particles

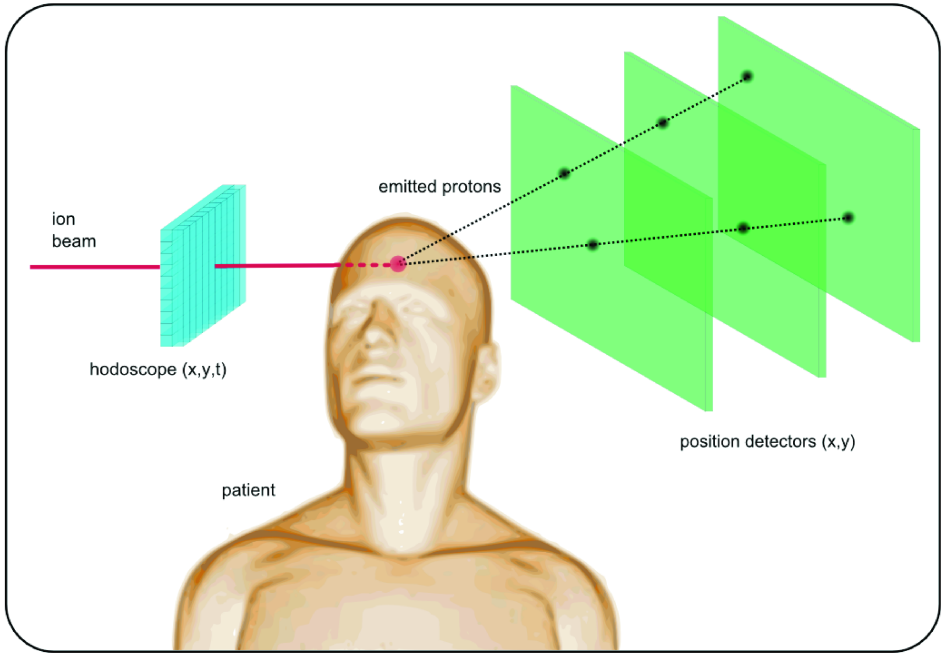

P. Henriquet PhD thesis, 2010,
Université Claude Bernard Lyon 1

Vertex distributions

GEANT4 Simulations

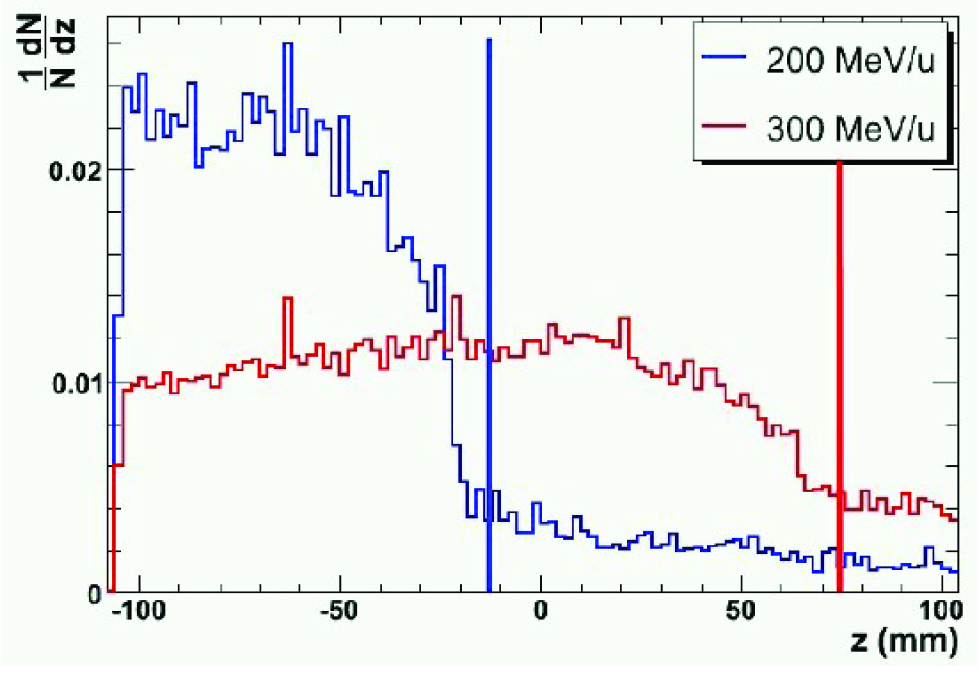

Clinical imaging

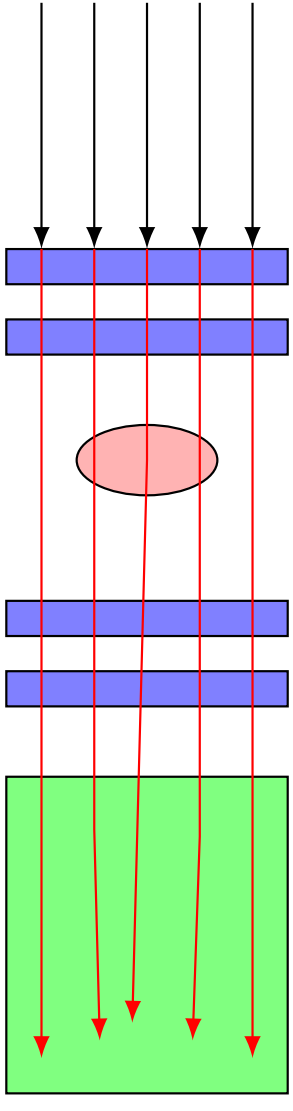

proton beam

position sensitive detector

range or energy detector

Clinical imaging

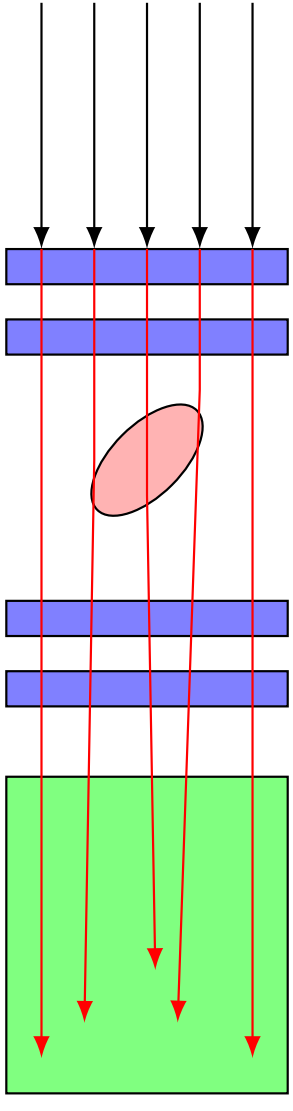

proton beam

position sensitive detector

range or energy detector

Clinical imaging

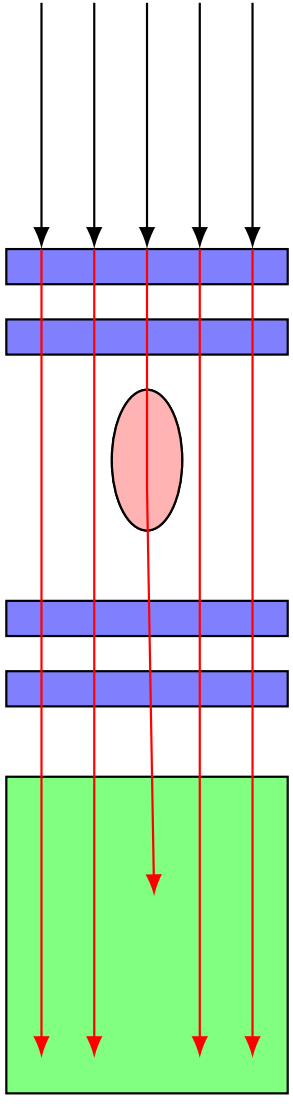

proton beam

position sensitive detector

range or energy detector

Clinical imaging

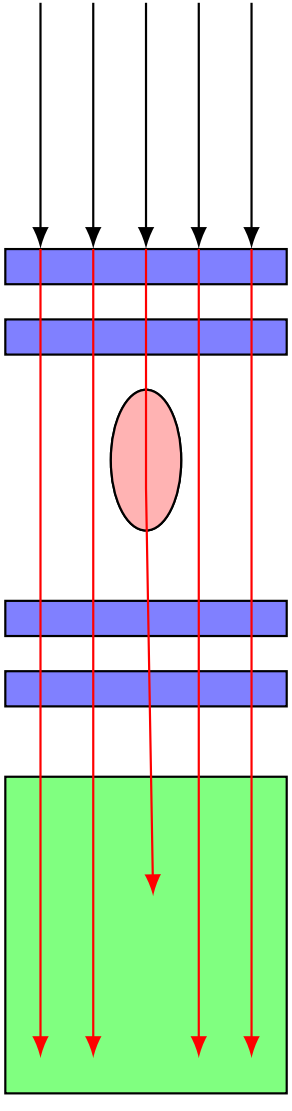

proton beam

position sensitive detector

range or energy detector

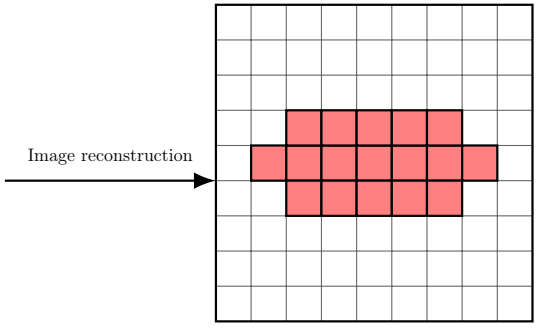

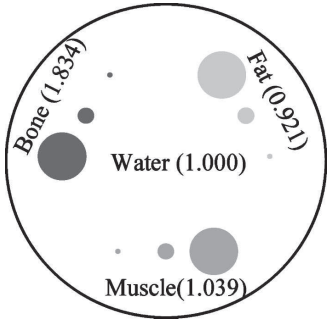

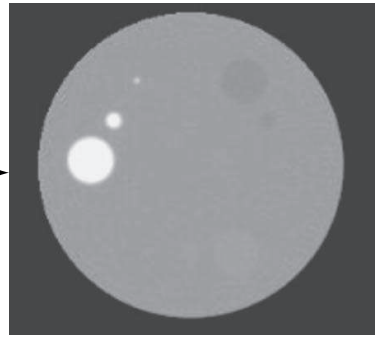

Schulte et al., Med. Phys. **32** *(2005) 1035.*

Higher accuracy, less dose!

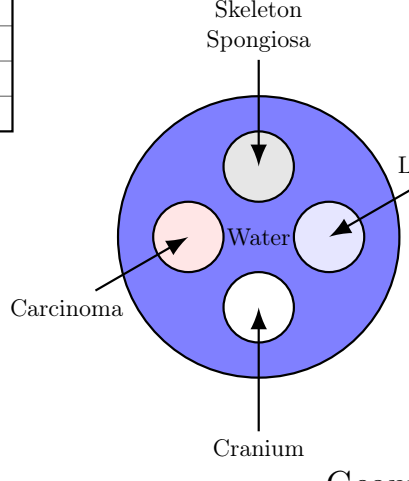

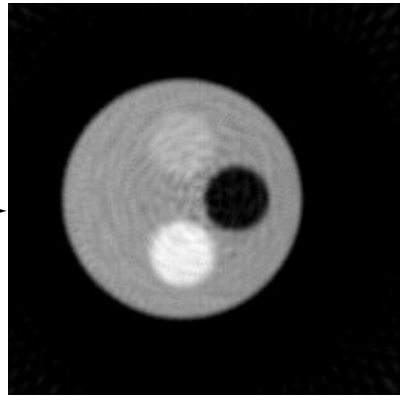

Geant4 simulation

Irradiating a sphere by using the spot scanning with proton beams

	1	2	3	4	5	6	7	8	9	10	11	12	13	14	15	16	17	18	19	20	21
1																					
2																					
3																					
4																					
5																					
6																					
7																					
8																					
9																					
10										0.691	0.174	0.691									
11										0.175	0.105	0.175									
12										0.691	0.175	0.691									
13																					
14																					
15																					
16																					
17																					
18																					
19																					
20																					
21																					

Beam fluence map

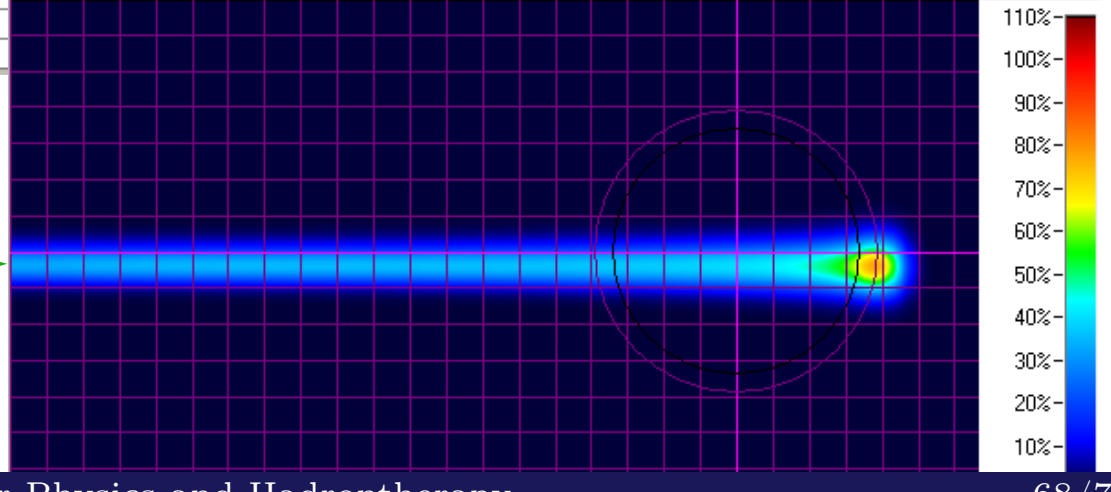

Dose map

Irradiating a sphere by using the spot scanning with proton beams

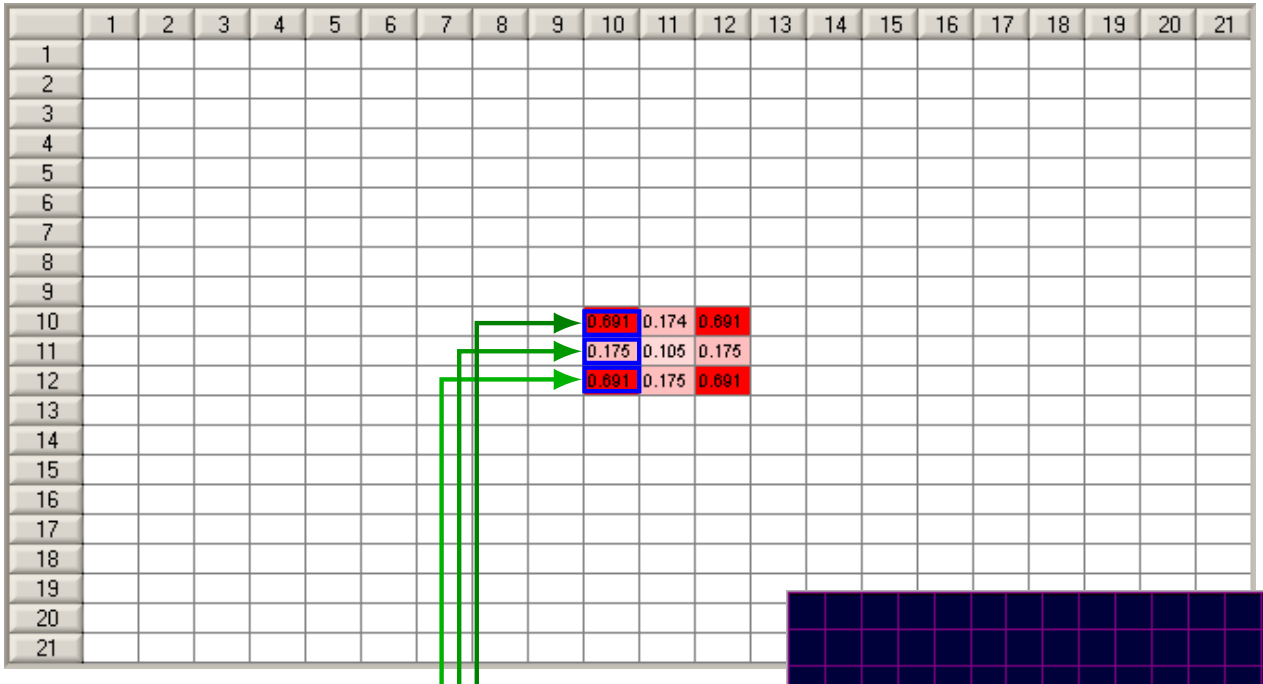

Beam fluence map

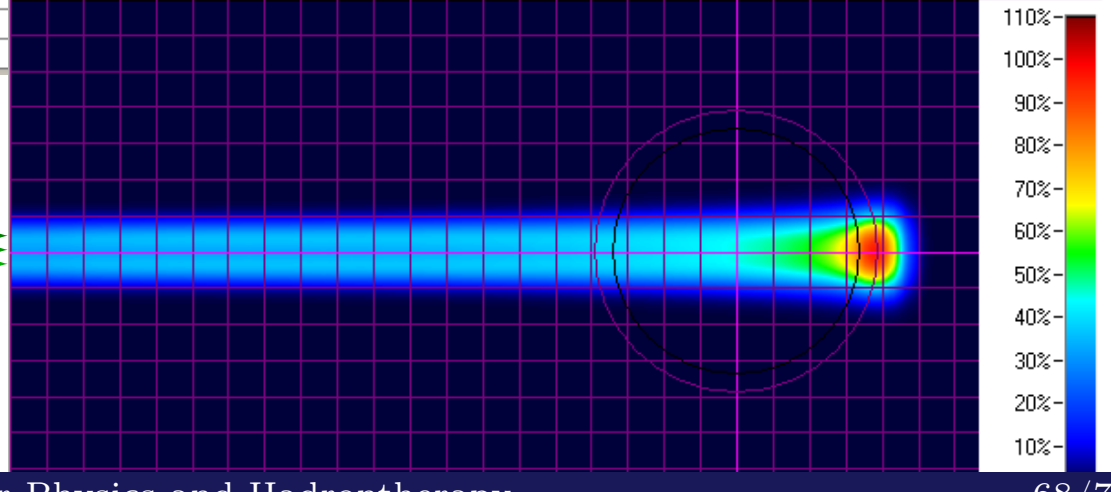

Dose map

Irradiating a sphere by using the spot scanning with proton beams (continued)

$N_{max} \approx 2.2\,10^6$

$N \approx 3.8\,10^5$

	1	2	3	4	5	6	7	8	9	10	11	12	13	14	15	16	17	18	19	20	21
1																					
2																					
3																					
4																					
5									0.281	0.347	0.333	0.345	0.281								
6								0.235	0.016	0.000	0.000	0.000	0.019	0.230							
7							0.229	0.013	0.000	0.000	0.000	0.000	0.000	0.014	0.230						
8						0.230	0.015	0.000	0.019	0.027	0.007	0.027	0.019	0.000	0.013	0.230					
9					0.282	0.018	0.000	0.021	0.059	0.067	0.059	0.066	0.058	0.019	0.000	0.019	0.280				
10					0.346	0.000	0.000	0.026	0.067	0.000	0.000	0.000	0.067	0.028	0.000	0.000	0.347				
11					0.333	0.000	0.000	0.005	0.060	0.000	0.159	0.000	0.061	0.006	0.000	0.000	0.334				
12					0.346	0.000	0.000	0.027	0.067	0.000	0.000	0.000	0.066	0.027	0.000	0.000	0.345				
13					0.281	0.019	0.000	0.020	0.059	0.068	0.060	0.067	0.059	0.018	0.000	0.017	0.282				
14						0.232	0.013	0.000	0.020	0.028	0.006	0.028	0.019	0.000	0.015	0.232					
15							0.230	0.015	0.000	0.000	0.000	0.000	0.000	0.015	0.227						
16								0.232	0.018	0.000	0.000	0.000	0.019	0.231							
17									0.281	0.347	0.334	0.346	0.283								
18																					
19																					
20																					
21																					

Beam fluence map

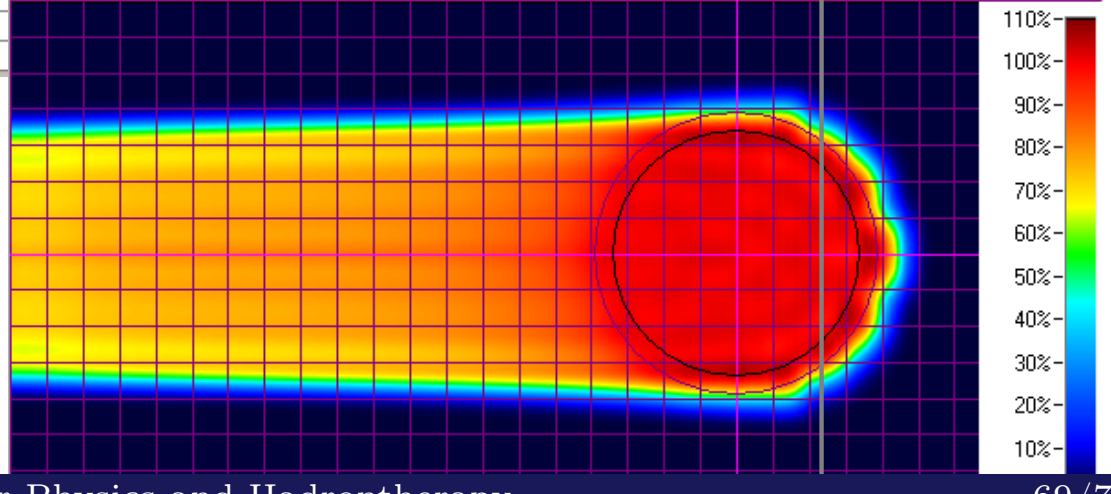

Dose map

Irradiating a sphere by using the spot scanning with proton beams (continued)

	1	2	3	4	5	6	7	8	9	10	11	12	13	14	15	16	17	18	19	20	21
1																					
2																					
3																					
4																					
5									0.070	0.058	0.046	0.060	0.071								
6								0.033	0.007	0.000	0.003	0.000	0.006	0.034							
7							0.027	0.000	0.007	0.008	0.012	0.010	0.005	0.000	0.029						
8						0.037	0.000	0.021	0.014	0.031	0.034	0.033	0.015	0.021	0.000	0.037					
9					0.070	0.006	0.006	0.017	0.000	0.016	0.013	0.016	0.000	0.016	0.006	0.006	0.071				
10					0.059	0.000	0.008	0.033	0.016	0.021	0.001	0.021	0.016	0.033	0.010	0.000	0.059				
11					0.046	0.004	0.015	0.031	0.012	0.002	0.006	0.002	0.012	0.032	0.013	0.005	0.046				
12					0.060	0.000	0.007	0.032	0.016	0.021	0.002	0.021	0.016	0.033	0.007	0.000	0.059				
13					0.069	0.005	0.005	0.015	0.000	0.016	0.012	0.016	0.000	0.016	0.005	0.006	0.071				
14						0.034	0.000	0.021	0.016	0.033	0.033	0.034	0.016	0.021	0.000	0.037					
15							0.028	0.000	0.004	0.008	0.012	0.008	0.006	0.000	0.028						
16								0.036	0.004	0.000	0.003	0.000	0.006	0.038							
17									0.070	0.059	0.045	0.058	0.071								
18																					
19																					
20																					
21																					

$N_{max} \approx 4.4\,10^5$

$N \approx 10^5$

Beam fluence map

Dose map

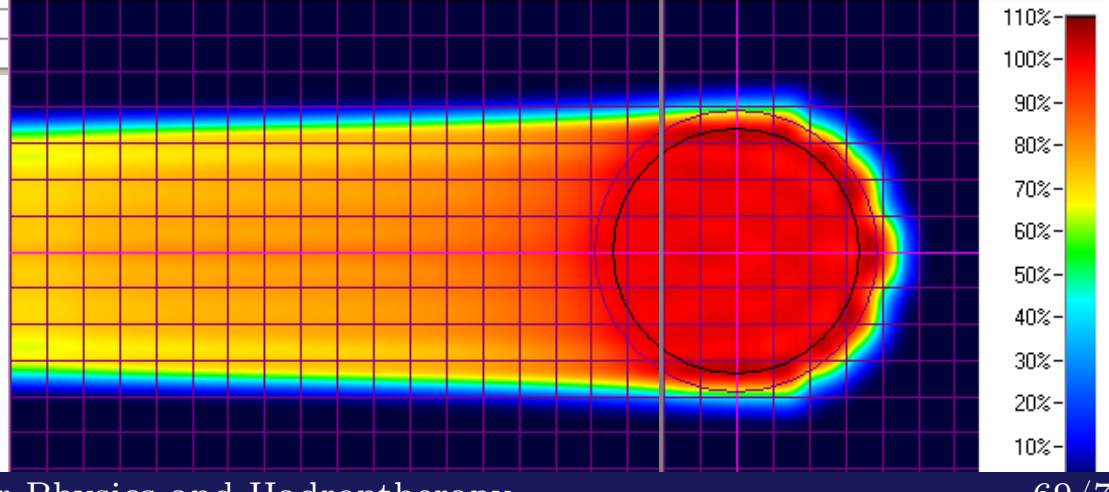

Beam monitor for hadrontherapy

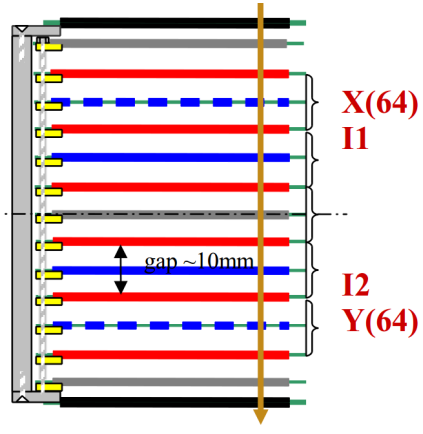

Water equivalent path:	200 μm
Beam location:	70 μm
Accuracy on fluency:	1.5 %

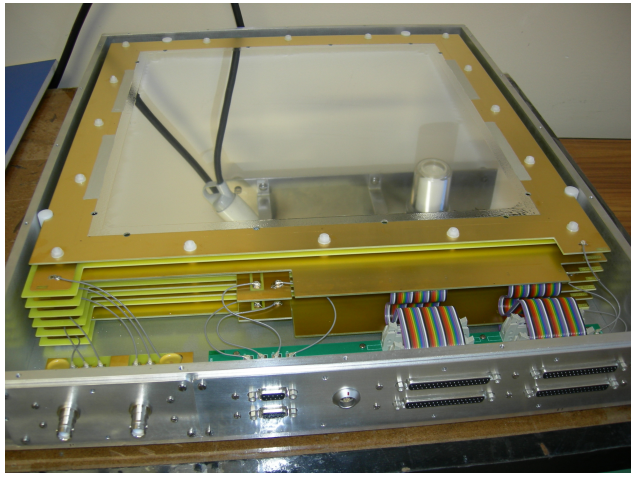

Charlotte Courtois PhD thesis

Tests ESSEN march & april & june 2009
"Westdeutsches Protontherapiezentrum Essen"
LPCCAEN - IBA collaboration

Accelerators for hadrontherapy

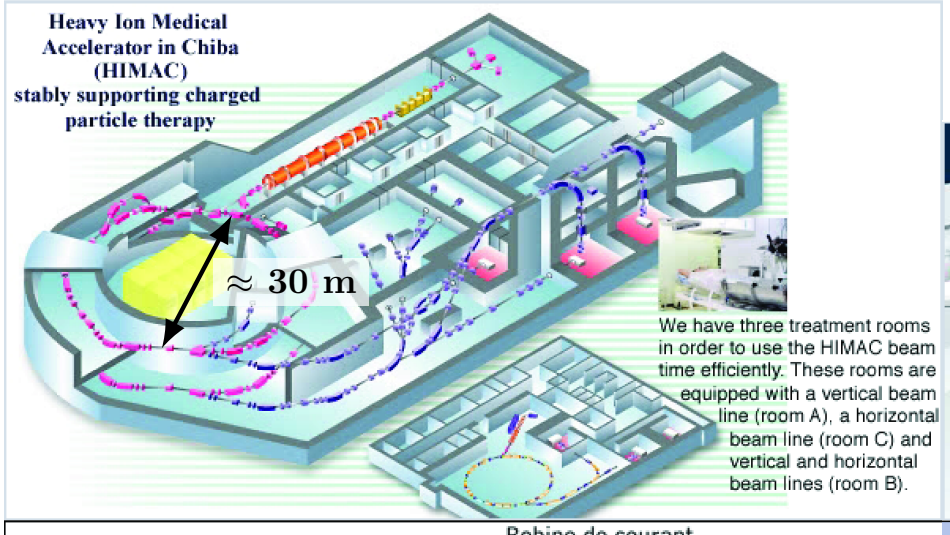

HIT-Heidelberg

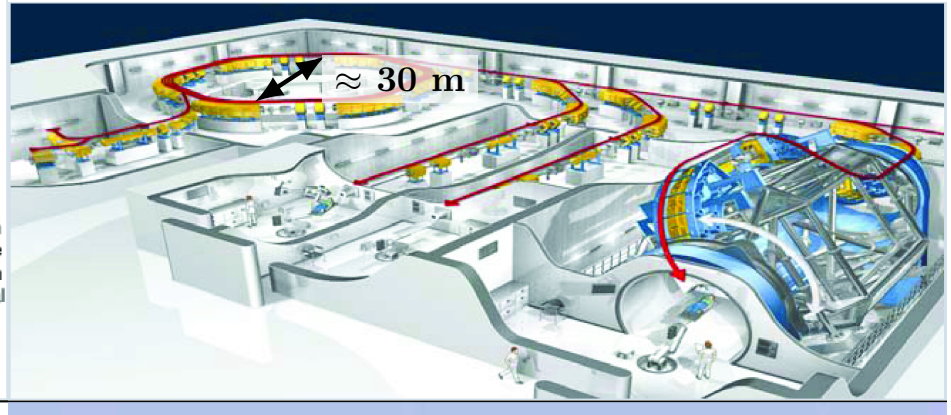

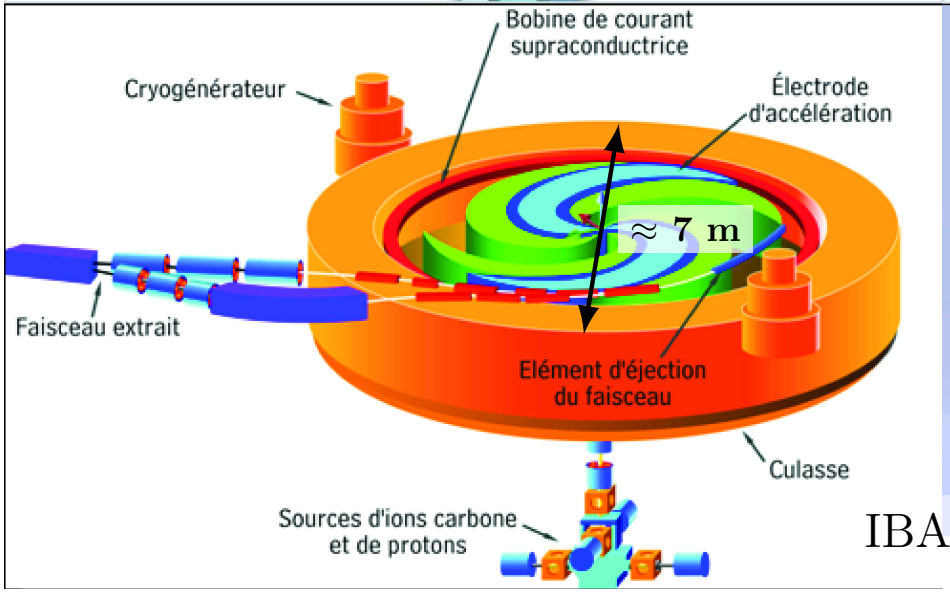

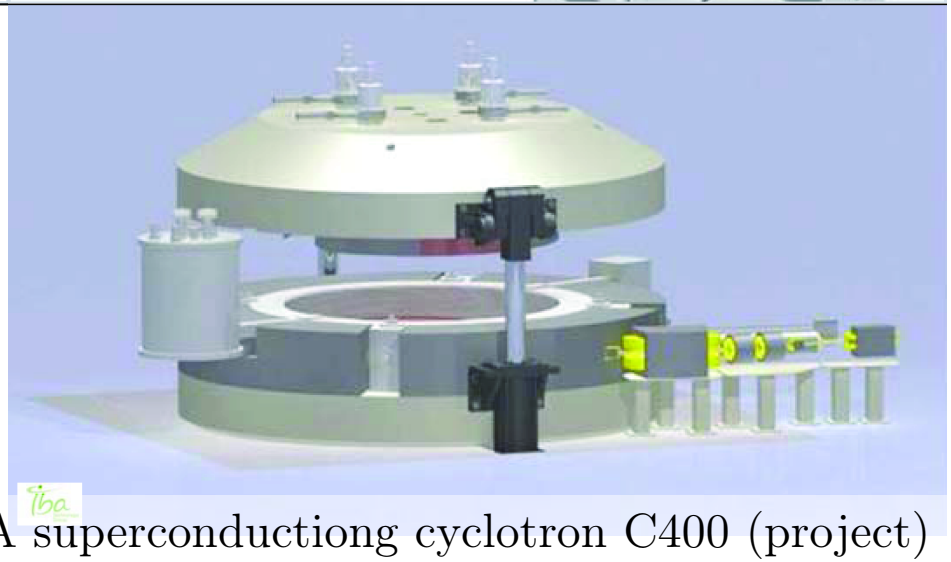

IBA superconductiong cyclotron C400 (project)

Contribution of nuclear physicists to the hadrontherapy

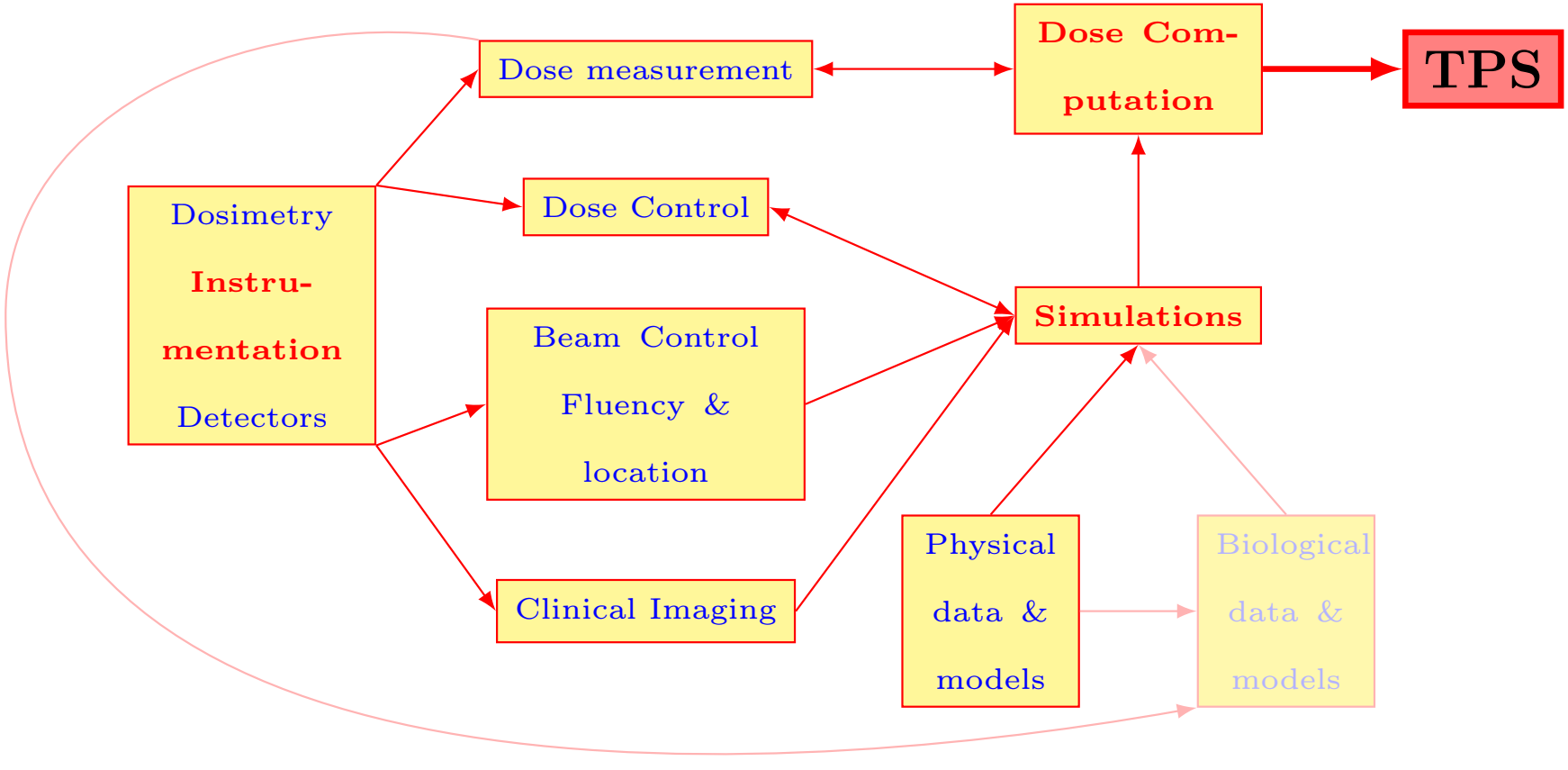

Final remarks

The hadrontherapy

- benefits from a good ballistics of heavy ions (Bragg Peak) and their good biological efficiency
- may help to cure resistant and non operable cancerous tumours
- needs heavy infrastructures to work (buildings, accelerators)
- is complementary to other therapies (chemotherapy, surgery, X-ray therapy)

The nucleus-nucleus collisions

- do not modify the range
- modify significantly the dose map
  - projectiles consumption $\longrightarrow \sigma_{reaction}$
  - lead to an energy deposition beyond the Bragg Peak ("fragmentation tail")
- may provide new tools to perform in-line dose controls $\longrightarrow$ nucleus-nucleus collision models

As a consequence

The nuclear physicist have a crucial role to play in optimizing the hadrontherapy by developping reliable nucleus-nucleus collision models and by providing innovative dosimetry devices.